ONTOGENY OF OROMANDIBULAR STRUCTURES IN THE ALGIVOROUS AND FEDERALLY THREATENED DEVILS RIVER MINNOW, *DIONDA DIABOLI*, WITH AN OVERVIEW OF KERATINIZED ORAL SURFACES IN NORTH AMERICAN MINNOWS (TELEOSTEI: CYPRINIDAE)

A Thesis

by

ILIANA MARIE MOCK

Submitted to the Office of Graduate and Professional Studies of
Texas A&M University
in partial fulfillment of the requirements for the degree of

MASTER OF SCIENCE

Chair of Committee,	Kevin W. Conway
Committee Members,	Delbert M. Gatlin, III
	Christopher D. Marshall
Head of Department,	Michael P. Masser

May 2017

Major Subject: Wildlife and Fisheries Sciences

Copyright 2017 Iliana Marie Mock

ABSTRACT

Algivory is a widespread phenomenon in aquatic animals that involves the consumption of nutrient poor algae. Algivorous fishes often exhibit several common morphological adaptations to contend with this type of diet, including an elongated alimentary tract and the presence of unicuspid or multicuspid teeth in dentulous fishes to facilitate removal of algae from the substrate. Keratinization of the epithelium covering the mouthparts has been hypothesized to facilitate oral scraping of algae from the substrate in the edentulous algivorous fishes of the family Cyprinidae (carps, minnows, and their relatives). Keratinization of the mouthparts has been well studied in Old World members of the Cyprinidae but remains understudied in the North American (New World) members of this successful group. This study represents the first to investigate the nature and extent of oral keratinization in the New World Members of the Cyprinidae. In the first part of this study, I use a combination of scanning electron microscopy (SEM) and histology to investigate the ontogeny of keratinization on the epithelium covering the jaw bones in *Dionda diaboli*, a federally threatened algivore that is currently the focus of a USFWS captive propagation program with high levels of mortality. Individuals of *D. diaboli* ≥9.0 mm SL exhibit a transverse band of keratinized epithelium covering the jaw bones. Histochemical investigation using A-S and H&E staining indicates that keratin is restricted to cells of superficial layer of the transverse band, which exhibit polygonal truncate unculi in individuals of 9.0-25.0 mm SL. In

larger individuals (≥25.0 mm SL), keratinized cells of the transverse band lack unculi and exhibit a flaky appearance. Expansion of the transverse band on the jaws occurs concurrently with elongation and coiling of the gut, and the addition of algal matter into the diet of hatchery individuals to coincide with the first appearance of a keratinized jaw epithelium could be beneficial to the captive rearing of this threatened species. In the second part of this study, I use SEM and histological techniques to investigate the nature and extent of oral keratinization in 55 species (representing 50 genera) of North American minnows, including members of both the 'Shiner' clade and the 'Western' clade. A phylogenetic comparative approach was used to investigate the relationship between the structure and length of the gut tract relative to oral keratinization in members of the 'Western' and 'Shiner' clades. Three general states of keratinized oral epithelia were observed among the species of North American minnow examined, including non-keratinized, keratinized squamous, and unculiferous. A non-keratinized epithelium was observed only in one species (*Hybognathus nuchalis*). The remaining character states were observed in both algivores and non-algivores, and a positive correlation was detected between gut coiling and keratinized oral epithelium within the 'Western' clade but not the 'Shiner' clade. No correlation exists between the percent of keratinized oral epithelium covering the surface of the jaws and gut length within the 'Western' clade but a negative correlation was detected between these two traits within the 'Shiner' clade. The high prevalence of keratinized oral surfaces in non-algivorous fishes suggests that this character may have more complex roles in the life history of many species.

DEDICATION

I dedicate this thesis work to my grandmother, Beverly Goodrum, and my mom, Karen Gonzales, for their continuous love and support throughout this project.

ACKNOWLEDGEMENTS

I would like to thank my advisor, Dr. Kevin Conway, for his support and valuable guidance throughout my graduate research and for helping me become a better writer. I also thank Dr. Delbert Gatlin and Dr. Christopher Marshall for serving as my committee members and Patricia Echo-Hawk for her help with obtaining samples of *Dionda diaboli* for my study.

I also thank Mike Pendleton and Tom Stephens for their patience and help learning specimen coating and SEM at the Microscopy and Imaging Center, Heather Prestridge at the Biodiversity Research and Teaching Collections, and the following museums for access to specimens of North American minnows: Bell Museum of Natural History, Florida Museum of Natural History, Natural History Museum of Los Angeles, New York State Museum, North Carolina Museum of Natural Sciences, Oregon State Museum of Biological Diversity, University of Alabama Ichthyological Collection, and the University of Michigan Museum of Zoology.

Thanks also go to my friends and colleagues, Amanda Pinion and Kole Kubicek, for all of their help and for making my time at Texas A&M University unforgettable.

CONTRIBUTORS AND FUNDING SOURCES

This work was supervised by a thesis committee consisting of Dr. Kevin W. Conway and Dr. Delbert M. Gatlin of the Department of Wildlife and Fisheries, and Dr. Christopher D. Marshall of the Department of Marine Biology at Texas A&M Galveston.

Specimens of *Dionda diaboli* analyzed for Chapter 1 were collected and preserved by Patricia Echo-Hawk at the U.S. Fish and Wildlife San Marcos Aquatic Resources Center. All other work conducted for the thesis was completed myself under the advisement of Dr. Kevin W. Conway of the Department of Wildlife and Fisheries. This research was funded by Texas A&M Agrilife Research.

TABLE OF CONTENTS

Page

LIST OF FIGURES

LIST OF TABLES

Page

CHAPTER I

INTRODUCTION

Algivory is a widespread phenomenon among many families of fishes and is often accompanied by morphological adaptations that facilitate the digestion and removal of low-nutrient algae from the substrate. A widely documented morphological condition among algivores is the presence of an elongated gut tract, which is hypothesized to increase digestive efficiency (German et. al 2006). While a number of algivorous fishes possess unicuspid (Uehara & Miyoshi 1993) or multicuspid teeth (Yamaoka 1983, Gibson 2015) to aid in scraping behaviors, a considerable number are edentulous and instead exhibit keratinized oral epithelia composed of minute unicellular projections arising from the surface of a single cell, known as unculi (singular unculus, *sensu* Roberts 1982), which have been previously documented among African and Asian algivores in the family Cyprinidae (Pinky et al. 2002, Tripathi & Mittal 2010). Unculi exhibit considerable variation in structure and size and are hypothesized to assist in scraping when located on the oral surfaces in fishes that obtain food items directly from the substrate (Pinky et al. 2002, Geerinckx et al. 2007, Roberts 1982).

Little information is known about these structures in the trophic morphology of algivorous North American minnows, many of which are threatened or endangered. The algivorous Devils River minnow (*Dionda diaboli* Hubbs & Brown 1957) is a federally threatened species of the North American Cyprinidae endemic to the spring-fed

tributaries of the central Rio Grande drainage of the United States and Mexico (Garrett et al. 2004, Hulbert et al. 2007). Little is known about the ecology and life history of *Dionda diaboli*, though its distribution is highly fragmented and it currently resides only within a few small creeks and rivers in I and potentially also Mexico (Garrett et al. 2004). As a result of its limited range and specific habitat requirements (i.e., fast-moving, clear, spring-fed waters), the Devils River minnow is considered vulnerable to further decline and the UFSWS is currently engaged in a captive breeding program for this species at the San Marcos Aquatic Resource Center (SMARC). The success of the captive breeding program at SMARC (as measured by the number of captive spawned individuals that make it to the adult stage) has remained low (~1.5% of larvae hatched reach the adult stage; Echo-Hawk 2015), despite ongoing refinement of captive propagation protocols (e.g., Gibson & Fries 2005). It is known that zooplanktivorous larvae undergo an ontogenetic dietary shift from planktivory to algivory that is accompanied by elongation of the gut (Hulbert et al. 2007, Gibson & Fries 2005, Echo-Hawk 2015) though it is unknown whether keratinized oral epithelium also occurs in conjunction with this ontogenetic shift and when such a adjustment begins to occur. Investigating the anatomy and development of the trophic apparatus of *Dionda diaboli* may not only be crucial to refining feeding regimes that increase hatchery yield, but may also provide insight into the process of keratinization of the oral jaws in a North American algivorous freshwater fish.

In addition to *Dionda*, North American is home to approximately 300 species of cyprinid fishes that exhibit a variety of different diets, trophic anatomy and life history

strategies (Gidmark & Simmons 2014). Many genera are comprised solely of obligate algivores, including members of *Achrocheilus* and *Campostoma* (Gidmark & Simmons 2014), though some primarily planktivorous genera also contain a small number of obligate algivores (e.g., *Notropis mekistocholas* Snelson 1971). Investigations of unculi in New World cyprinids are restricted to a small number of taxa, including the archetypal North American algivore *Campostoma* (Roberts 1982), though the diversity of different diet types present within the North American minnow clade presents an ideal opportunity to further investigate the roles of oral keratinization and unculi in algivorous fishes.

In the first part of this study, to use a combination of scanning electron microscopy (SEM) and histological techniques to: (1) document the anatomy of the oral jaws in *D. diaboli*; (2) assess whether the oral jaw surfaces of *D. diaboli* are keratinized; and (3) assess the interplay between oral keratinization and gut elongation throughout ontogeny. In the second part of this study, I use a combination of SEM, histological techniques, and phylogenetic comparative methods to investigate the distribution and evolution of oral keratinization in 55 species of North American minnows representing 50 genera in order to assess whether a general relationship exists between oral keratinization and algivory in North American minnows.

Based on previous recordings of vast numbers of unculi on the jaw epithelium of Old World algivorous cyprinids (Roberts 1982, Pinky et al. 2002, Tripathi & Mittal 2010), I predict that that a keratinized mechanism for algivorous feeding is likely present in *Dionda diaboli* and other North American minnows as it may confer a selective

advantage regarding foraging behavior. I also predict that gut elongation (a common adaptation for algivory; German et al. 2006) and the development of oral unculi will coincide in the ontogeny of *Dionda diaboli*, and that the most substantial degree of oral keratinization and gut elongation will be observed among the North American minnow genera that currently exhibit algivorous foraging behavior.

CHAPTER II

ONTOGENY OF *DIONBDA DIABOLI*

2.1 Introduction

The Devils River minnow (*Dionda diaboli* Hubbs & Brown 1957) is a species of the Cyprinidae (order Cypriniformes) endemic to the spring-fed tributaries of the central Rio Grande drainage of the United States and Mexico (Garrett et al. 2004; Hulbert et al. 2007). The distribution of *D. diaboli* is highly fragmented and it currently resides only within a few small creeks and rivers in Texas, including Pinto creek, San Felipe Creek, and the Devils River, and is potentially extirpated from Las Moras creek and Sycamore creek (Garrett et al. 2004). Historic records indicate that *D. diaboli* also was present in several south bank tributaries to the Rio Grande in Mexico, including the Rio San Carlos and Rio Sabinas, though its status in Mexico is currently uncertain and it is thought to have been extirpated from these localities (Garret et al. 2002). The marked decline in this species has been attributed to human-induced loss of habitat and reduction of water flow, in addition to impacts from introduced species (Garrett et al. 2004; Hulbert et al. 2007). As a result of its limited range and specific habitat requirements (i.e., fast-moving, clear, spring-fed waters), the Devils River minnow is considered vulnerable to further decline and is currently listed as threatened by the U.S. Fish and Wildlife Service (USFWS) (USFW 1999, 2007).

Continuously dwindling numbers in wild populations have rendered *Dionda diaboli* a target species for captive propagation within the framework of the USFWS Endangered species recovery program. Currently, USFWS maintains multiple refugia populations of *D. diaboli* at the San Marcos Aquatic Resource Center (SMARC), representing multiple genetically distinct populations from throughout the Texas range of the species. Though individuals of *D. diaboli* spawn frequently within captivity, the success of the captive breeding program at SMARC, as measured by the number of captive spawned individuals that make it to the adult stage, has remained low (~1.5% of larvae hatched reach the adult stage; Echo-Hawk 2015), despite continuing refinement of captive propagation protocols (e.g., Gibson & Fries 2005).

Little is known about the ecology and life history of *Dionda diaboli.* In the wild, adult individuals forage directly from the substrate and have been referred to as herbivorous (Cohen 2008) or as obligate algivores (López-Fernández & Winemiller 2005), though larvae are zooplanktivorous and feed directly from the water column (Gibson & Fries 2005, Echo-Hawk 2015). This ontogenetic dietary shift from planktivory to algivory is accompanied by elongation of the gut (Hulbert et al. 2007; Echo-Hawk 2015), which is presumably an adaptation for increasing digestive efficiency (German & Horn 2006). In addition to possessing elongate guts, algivorous fishes frequently exhibit trophic modifications that facilitate removal of algae directly from the substrate. Most frequently, this involves modification of the oral jaw teeth to result in a dentition comprising high numbers of unicuspid (Uehara & Miyoshi 1993) or multicuspid teeth (Yamaoka 1983, Gibson 2015), but may also involve keratinization of

the lips and/or epithelium covering the oral jaw bones in edentulous fishes (Roberts 1982). Detailed morphological investigations of the edentulous and algivorous African and Asian cyprinid fishes using scanning electron microscopy (SEM) have documented high numbers of unculi (minute, keratinous projections arising from the surface of epidermal cells; *sensu* Roberts 1982) on the epithelium covering the edentulous jaw bones that are hypothesized to function as an abrasive device for the removal of algae from the substrate in the absence of oral jaw teeth (Roberts 1982, Pinky et al. 2002). Little information is available on the trophic morphology of the algivorous North American minnows, including *Dionda*, but unculi have been documented at least in the archetypal North American algivore *Campostoma* (Roberts 1982).

Documenting the anatomy and development of the trophic apparatus of the Devils River minnow could provide further insight into the algivorous lifestyle of this threatened species and potentially generate information with which to refine artificial feeding regimes within hatcheries, specifically the point at which algae is introduced to the diet, which has been shown to be crucial for successful rearing (Echo-Hawk 2015). In this investigation, I use a combination of scanning electron microscopy and histological techniques to: (1) document the anatomy of the oral jaws in *D. diaboli*; (2) assess whether the oral jaw surfaces of *D. diaboli* are keratinized; and (3) assess the interplay between oral keratinization and gut elongation throughout ontogeny.

2.2 Materials and Methods

Specimens of *Dionda diaboli* utilized in this study were obtained from the captive-breeding program at the USFWS San Marcos Aquatic Resources Center (SMARC) located in San Marcos, Texas. Specimens were sampled daily between 1-36 days post hatch (dph), and at 6 months and 1 year of age. Upon collection, individuals were euthanized via an overdose treatment of tricaine methanesulfonate (MS222) and fixed in a solution of 10% buffered formalin for 24 hours before being transferred via a graded series of ETOH (30%, 50% and 70%) to 70% EtOH for final storage. Once in 70% ETOH, specimens were measured (using an ocular micrometer attached to a ZEISS STEMI 2000 stereomicroscope and sorted into size classes of 7.0 mm, 9.0 mm, 10.0 mm, 15.0 mm, 22.0 mm, and 25.0 mm standard length (SL). Individuals in size classes below 10.0 mm SL are referred to as larvae and those between 10.0-25.0 mm SL are referred to as juveniles in accordance with previous ontogenetic work on *D. diaboli* (Hulbert et al. 2007). Specimens below 7.0 mm possess a yolk sac (Hulbert et al. 2007) and were not examined. Specimens collected at 6 months and 1 year of age were classified as adults and are referred to herein by their respective age (6 months or 1 year) instead of by length due to the wide variation in SL exhibited by the individuals examined representing these age classes (34.0-39.0 mm SL for 6 month old individuals; 31.0-33.0 mm SL for one year old individuals). Additional wild-caught individuals of *D. diaboli* and other species of *Dionda* housed in museum collections (see list of materials examined) were also investigated.

2.2.1 Scanning Electron Microscopy

The head of two individuals from each size class and one head from each age class were removed from the body. The head of one individual from each size and age class was dissected along the coronal plane into dorsal and ventral halves containing the upper and lower jaws, respectively. Separation of each head was initiated at the corners of the mouth and continued posteriorly through the junction of the ceratobranchials and epibranchials to expose the inner surfaces of the buccal cavity for scanning electron microscopy (SEM) investigation. Specimens were chemically dried using the protocol of Ellis & Pendelton (2007), affixed to pin mounts with carbon tape, coated with gold in a vacuum sputter coater (Technics Hummer 1) and examined using a TESCAN Vega 3 environmental scanning electron microscope. Digital photographs obtained were processed, edited, and analyzed using Adobe Photoshop and Adobe Illustrator CS5.1.

2.2.2 Serial Sectioning

The heads of three individuals from each size class and two from each age class were removed from the body, decalcified (following Conway et al. 2012), dehydrated through a series of EtOH and then subsequently cleared in toluene before being embedded in paraffin. Embedded heads were then sectioned sagittally (7 μm) using a Spencer 820 rotary microtome. Sections were mounted on glass slides and stained with hematoxylin and eosin (H&E) (2 heads) following the procedures of Kiernan (1990) or Ayoub-Shklar stain (A-S) (1 head) for keratin following Ramulu et al. (2013). Slides were examined and photographed using a ZEISS Primo Star compound light microscope

equipped with an AxioCam MRc5 digital camera. Digital photographs were processed, edited, and analyzed using Adobe Photoshop and Adobe Illustrator CS5.1.

2.2.3 Gross Examination of the Alimentary Canal

The post-pharyngeal alimentary canal was removed from the body of dissected specimens, uncoiled if necessary, and measured (without stretching) to the nearest 0.01 mm using an ocular micrometer attached to a ZEISS SteREO Discovery V20 stereomicroscope. Dissected alimentary canals were classified as either straight (no bending occurs between the mouth and anus), s-shaped (two distinct bends), or coiled (multiple bends).

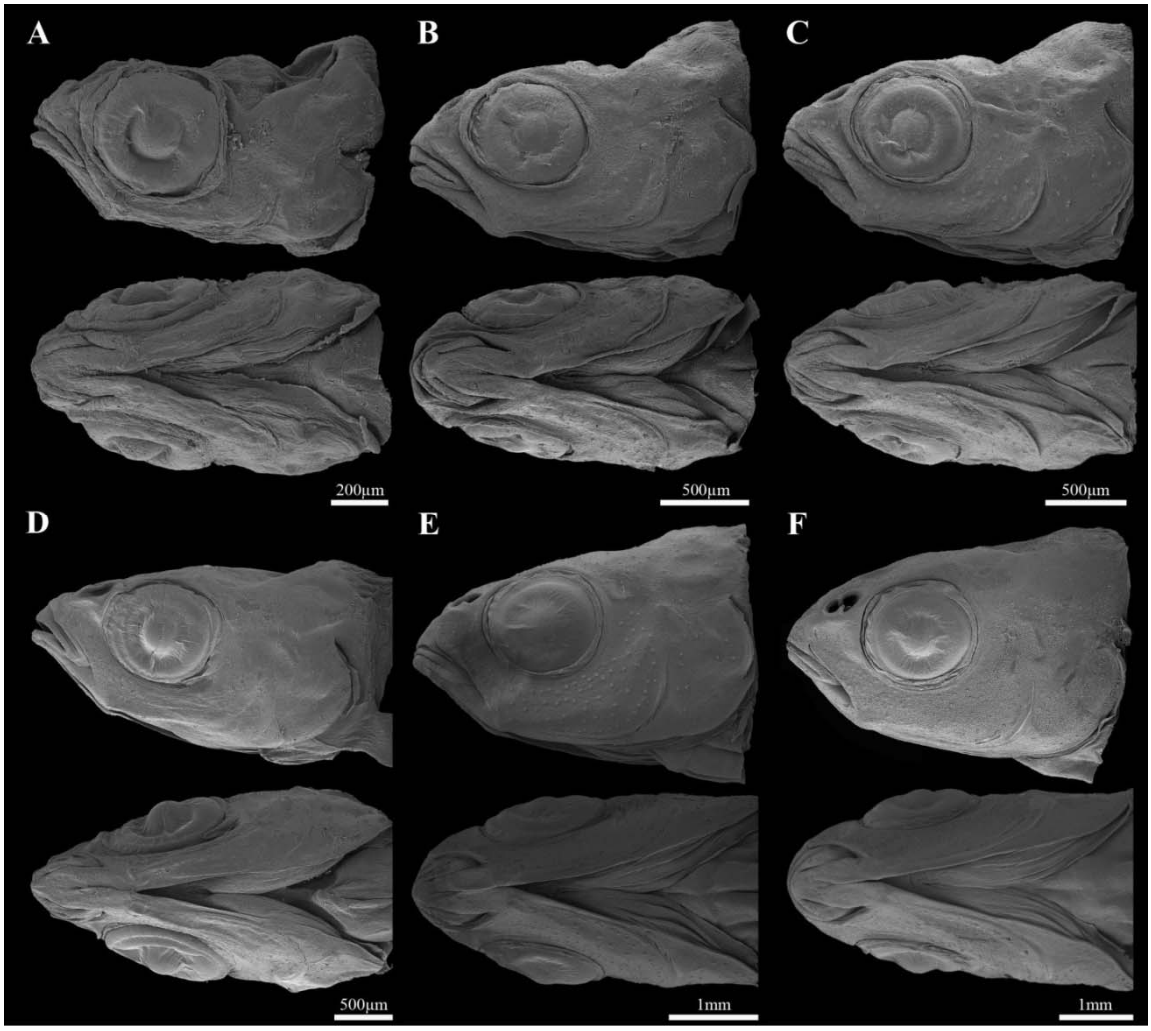

Figure 2-1. Scanning electron micrographs of the complete excised heads of *Dionda diaboli* larvae and juveniles. (**A**) 7.0 mm SL larvae. (**B**) 9.0 mm SL larvae. (**C**) 10.0 mm SL juvenile. (**D**) 15.0 mm SL juvenile. (**E**) 22.0 mm SL juvenile. (**F**) 25.0 mm SL juvenile. Mouth position remains terminal throughout ontogeny until approximately 22.0 m SL wherein a slight subterminal position is observed. No unculi are evident from the outside.

2.3 Results

2.3.1 7.0 mm SL

Larvae of this size (n=5) exhibit a terminal mouth with a weakly developed rostral groove dorsal to the center of the upper lip (Figure 2-1A). Superficial cells of the epithelia covering the lips and jaws exhibit a plicate surface centrally with slightly raised borders (Figure 2-2A,D). There is no sign of keratinization on the epithelium of the lips or jaws as revealed by A-S or H&E staining (Figure 2-3A,B). The alimentary canal is represented by a straight tube.

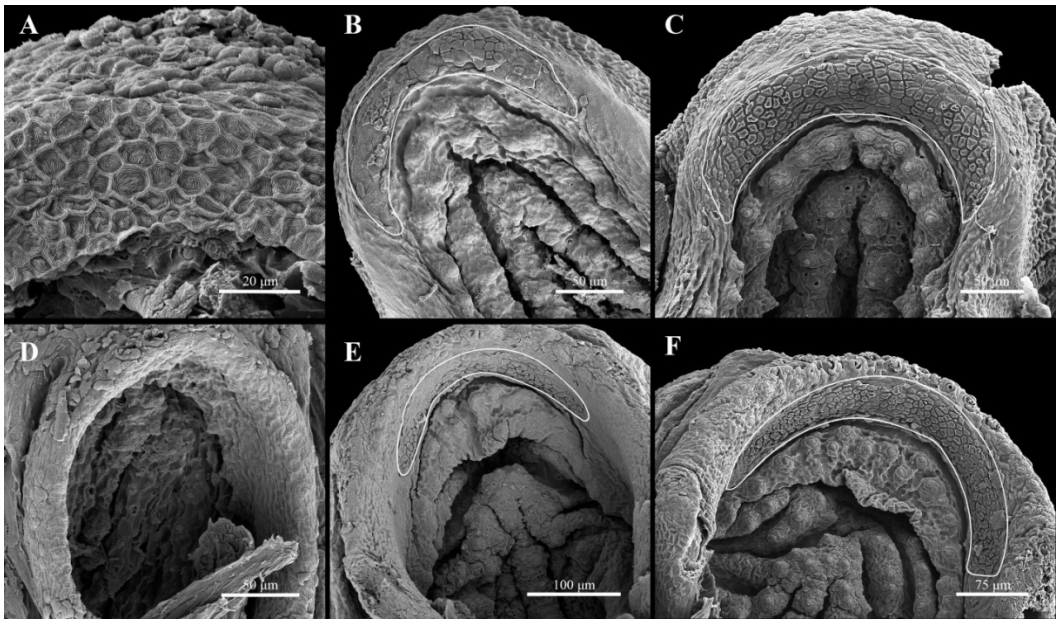

Figure 2-2. Scanning electron micrographs of the inner surfaces of the lower and upper jaws of larval and juvenile *Dionda diaboli*. (**A**) Close-up of the inner curvature of the lower jaw in a 7.0 mm SL larvae. (**B**) Inner surface of the lower jaw on a 9.0 mm SL larvae. (**C**) Inner curvature of the lower jaw on a 10.0 mm SL juvenile. (**D**) View of the inner surface of the upper jaw of a 7.0 mm SL larvae. (**E**) View of the inner curvature of the jaw on a 9.0 mm SL larvae. (**F**) Inner curvature of the jaw on a 10.0 mm SL juvenile. Keratinization is not yet visible on the 7.0 mm SL specimen, though epithelial cells on the lips appear concave with raised edges. The first true unculi are visible on the 9.0 mm SL larvae, and have expanded laterally outward in the 10.0 mm SL juvenile. Outlined areas indicate the keratinized sheath of unculi forming on the 9.0 mm and 10.0 mm individuals.

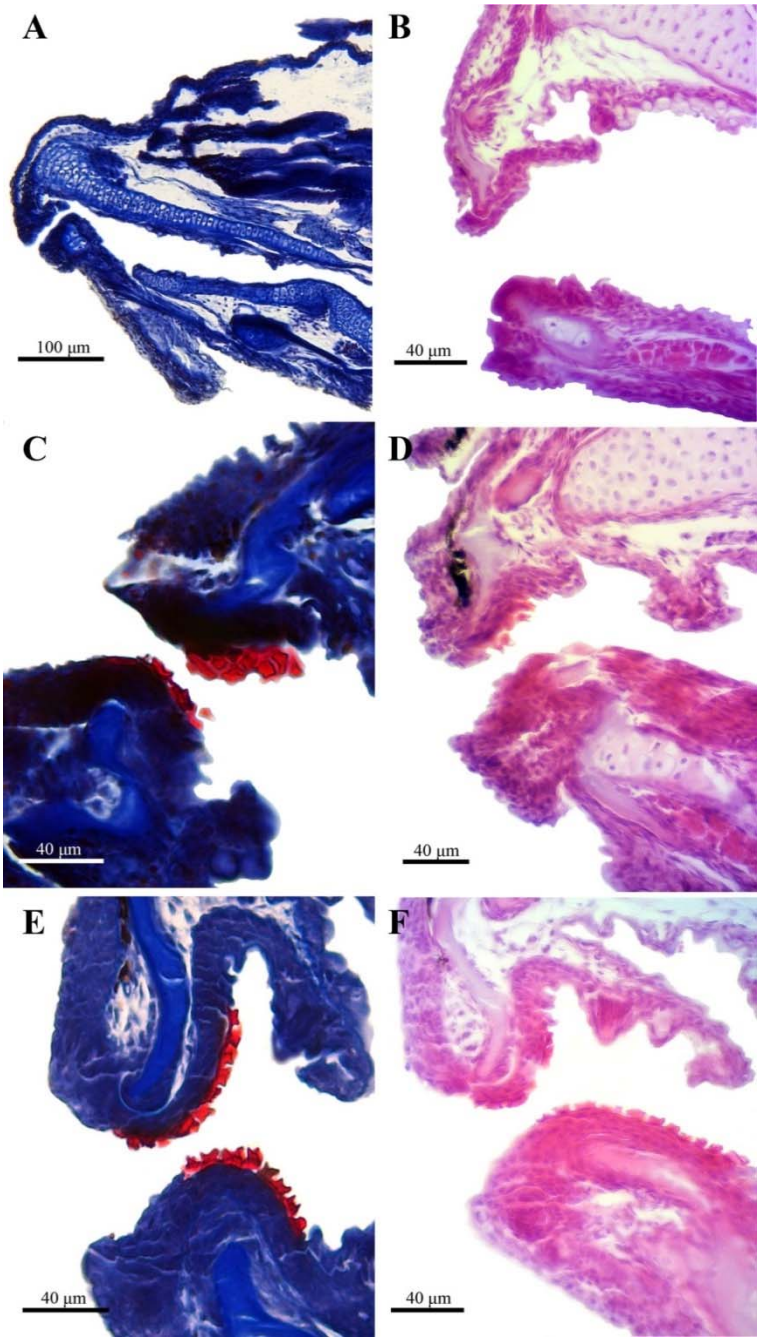

Figure 2-3. Sagittal sections of larval and juvenile *Dionda diaboli*. (**A**) Anteriormost head region of a 7.2 mm SL larvae stained via A-S. (**B**) Upper and lower jaws of a7.0 mm SL larvae with H&E staining. (**C**) Upper and lower jaws of a 9.0 mm SL larvae with A-S stain. (**D**) Upper and lower jaws of a 9.0 mm SL larvae with H&E staining. (**E**) Upper and lower jaws of a 10.0 mm SL juvenile with A-S stain. (**F**) Upper and lower jaws of a 10.0 m SL juvenile with H&E staining. Unculi become visible among 9.0 mm individuals and initially display a molar-like appearance; individuals below 9.0 mm SL show no evidence of counterstain.

2.3.2 9.0 mm SL

Larvae of this size (n=5) exhibit a terminal mouth with a distinct rostral groove bordering the entire dorsal margin of the upper lip (Figure 2-1B). Superficial cells of the epithelium located around the periphery of the upper and lower jaws exhibit plicate surfaces without raised borders (Figure 2-2B,E). Superficial cells at the center of the epithelium covering the upper and lower jaws lack microplicae and exhibit a polygonal projection arising from the cell surface. The rugose outer margin of each polygonal projection surrounds a concave central depression (Figure 2-2B,E). Superficial cells with polygonal projections are arranged in a narrow transverse band along the center of both the upper and lower jaw epithelia, covering approximately 24% and 32% of the surface of the upper and lower jaw epithelia, respectively (Figure 2-2B,E; Table 2-1). The surface projection of each of these cells stains deep red with A-S stain and bright pink with eosin (Figure 2-3C,D), indicating the presence of keratin. Cells of the epithelial layers immediately below the superficial layer of keratinized cells to the basement membrane are cuboidal and stain faintly with eosin and A-S. The alimentary canal is represented by a straight tube.

2.3.3 10.0 mm SL

Juveniles of this size (n=5) exhibit a terminal mouth and a pronounced rostral groove is visible along the entire dorsal curvature of the upper lip (Figure 2-1C). Superficial cells of the epithelium located around the periphery of the upper and lower jaws exhibit plicate surfaces with no raised borders. The distinct transverse band of superficial cells with polygonal surface projections that is present along the center of

Table 2-1. Measures of keratin coverage and gut length in accordance with standard length.

		Standard length class (mm)						Age class		
		Larvae		Juveniles				Adults		
		7.0	**9.0**	**10.0**	**15.0**	**22.0**	**25.0**	**6 month**	**1 year**	**Wild caught(n=1)**
Standard length (SEM individual)		7.0	9.0	10.0	15.0	22.0	25.0	38.87	31.35	53.21
Standard length (average of all individuals)		7.0	9.0	10.0	15.0	22.0	25.0	36.84	31.83	53.21
Epithelium type		non-keratinized	polygonal truncate unculi					keratinized squamous		
Keratin coverage per jaw	*Upper*	0	0.2435	0.2995	0.3464	0.4306	0.3725	0.4387	0.4390	0.5753
(SEM individual)	*Lower*		0.3189	0.3873	0.5761	0.4962	0.5694	0.6267	0.6218	0.6495
Total percent oral coverage (SEM individual)		0	0.2812	0.3434	0.4613	0.4634	0.4710	0.5327	0.5304	0.6124
Gut type		straight		S-shaped		coiled				
Gut % of SL (*n* =1, SEM individual)		0.44	0.40	0.46	0.74	1.09	1.52	2.62	1.89	2.60
Gut % of SL (average of all individuals)		0.44	0.40	0.65	0.65	1.08	1.59	2.62	2.09	2.60
% Eye-lateral head surface		0.3625	0.2018	0.2097	0.1947	0.1692	0.1456			

the epithelia covering the upper and lower jaws in smaller specimens now occupy a larger area, approximately 30% and 39% of the upper and lower jaw epithelia, respectively (Figure 2-2C,F; Table 2-1). The polygonal projection on the surface of each superficial cell contributing to the transverse band on the jaw epithelia stain deep-red with A-S stain and bright pink with eosin, indicating the presence of keratin (Figure 2-3E,F). Cells of the epithelial layers immediately below the superficial layer of keratinized cells to the basement membrane are cuboidal and stain weakly with eosin and A-S. The alimentary canal is represented by an s-shaped tube, with the middle segment of the intestine (between the initial and terminal bends) shorter in length than the foremost and hindmost segments.

2.3.4 15.0 mm SL

Features of the mouth and rostral groove in juveniles of this size (n=4) (Figure 2-1D) are similar to that described above for juveniles of 10 mm SL. Superficial cells of the epithelium covering the inner and outer periphery of the upper and lower jaws exhibit a flat surface with well-developed microplicae. The transverse band of superficial cells with polygonal surface projections present in the epithelia covering the center of the jaws in smaller specimens now occupies approximately 35% and 58% of the upper and lower jaw epithelia, respectively (Table 2-1). The central concave depression of each polygonal projection is less pronounced compared to the condition in smaller specimens. The polygonal projections on the surfaces of the superficial cells contributing to the transverse bands stain intensely with eosin, confirming that they are

keratinized. Cells of the epithelial layers immediately below the superficial layer of keratinized cells to the basement membrane are cuboidal and do not stain with eosin (Figure 2-4A). The alimentary canal is s-shaped. The anterior and middle segments of the canal are roughly equal in length and slightly shorter than the terminal segment.

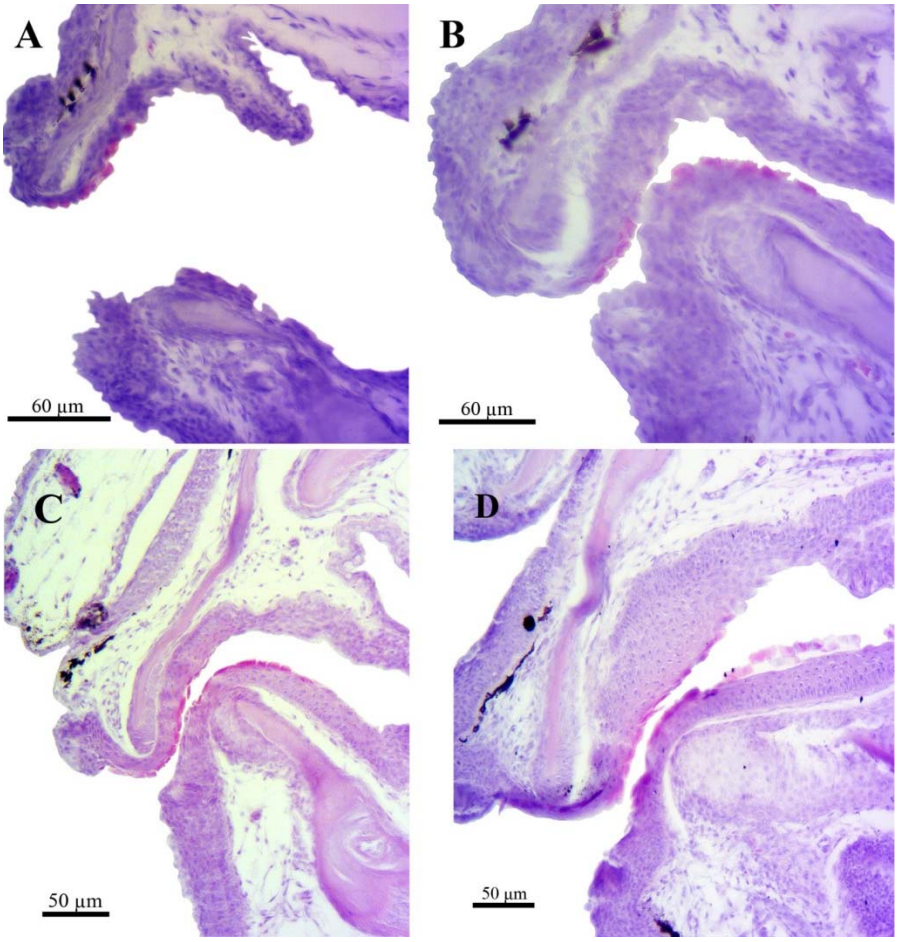

Figure 2-4. Sagittal sections of the upper and lower jaws of juvenile and adult *Dionda diaboli* using H&E staining. (**A**) 15.0 mm juvenile. (**B**) 22.0 mm SL juvenile. (**C**) 25.0 mm SL juvenile. (**D**) One year old adult. Unculi are observable on the inner curvatures of the upper and lower jaws and appear to decrease in height as aging progresses, appearing as flattened, squamous cells by the adult phase.

2.3.5 22.0 mm SL

Juveniles of this size (n=4) exhibit a slightly subterminal mouth with a well-developed rostral groove and cap. The rostral cap is larger relative to the previous size class, extending farther over the rostral groove toward the dorsal surface of the upper lip (Figure 2-1E). Superficial cells of the epithelium covering the inner and outer periphery of each jaw exhibit a flat surface with well-developed microplicae. The transverse band of keratinized, superficial cells present in the epithelium covering the center of each jaw in smaller specimens now occupies approximately 43% and 50% of the upper and lower jaw epithelia, respectively (Table 2-1). The central concave depression of the polygonal projection on the surface of superficial cells contributing to the transverse band is only weakly developed compared to the condition in smaller specimens (Figure 2-6A). The polygonal projections continue to stain intensely with eosin, signaling the presence of keratin. Cells of the epithelial layers immediately below the superficial layer of keratinized cells to the basement membrane are cuboidal and do not stain with eosin (Figure 2-4B). The medial segment of the alimentary canal extends anteriorly in the body cavity forming a loose, s-shaped loop. The anterior and posterior segments of the canal are straight.

2.3.6 25.0 mm SL

Juveniles of this size (n=4) possess a slightly subterminal mouth with a well-developed rostral groove and cap resembling an adult (Figure 2-1F). Features of the epithelium covering the upper and lower jaws are very similar to that described above

for juveniles of 22.0 mm SL except that transverse band of keratinized superficial epithelial cells present in the epithelium covering the center of each jaw now occupy approximately 37% and 57% of the upper and lower jaw epithelia, respectively (Table 2-1). The medial segment of the alimentary canal extends anteriorly within the body cavity in a tightly curled, s-shaped loop forming the coils of the intestine. The anterior and posterior segments of the canal are straight.

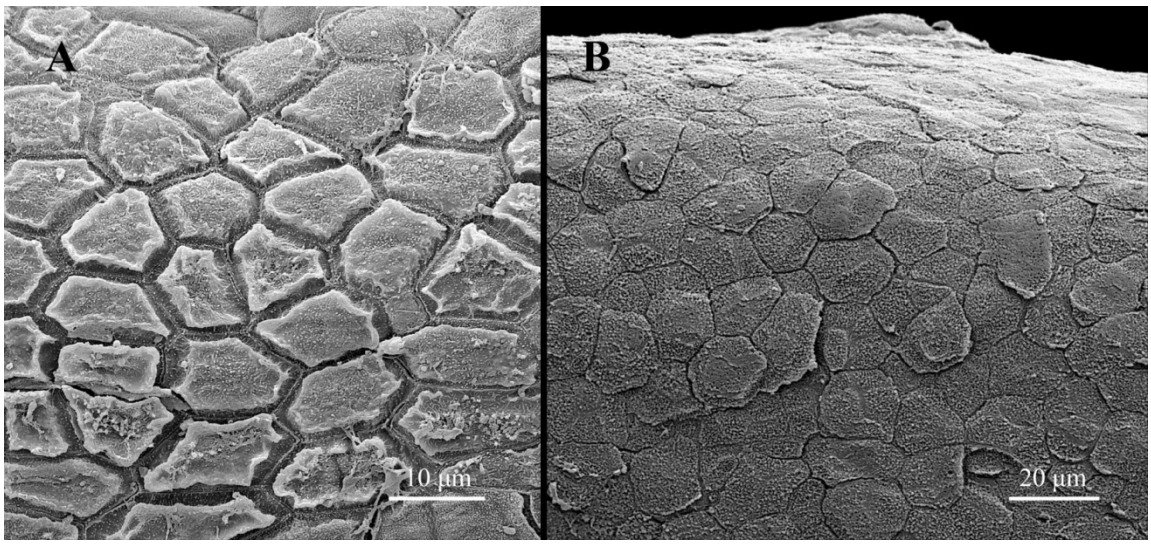

Figure 2-5. Close-ups of keratinized oral tissue comparing cell height and cell surface texture. (**A**) Raised polygonal unculi in a 22.0 mm specimen. (**B**) Squamous keratinized cells in a 6 month individual.

2.3.7 Adults

Adults of approximately 6 months (n=3) and 1 year (n=3) of age and an additional wild-caught adult of unknown age (n=1) exhibit a subterminal mouth with a well-developed rostral groove and cap. The superficial cells of the epithelium covering the inner and outer periphery of each jaw exhibit a flat surface with well-developed

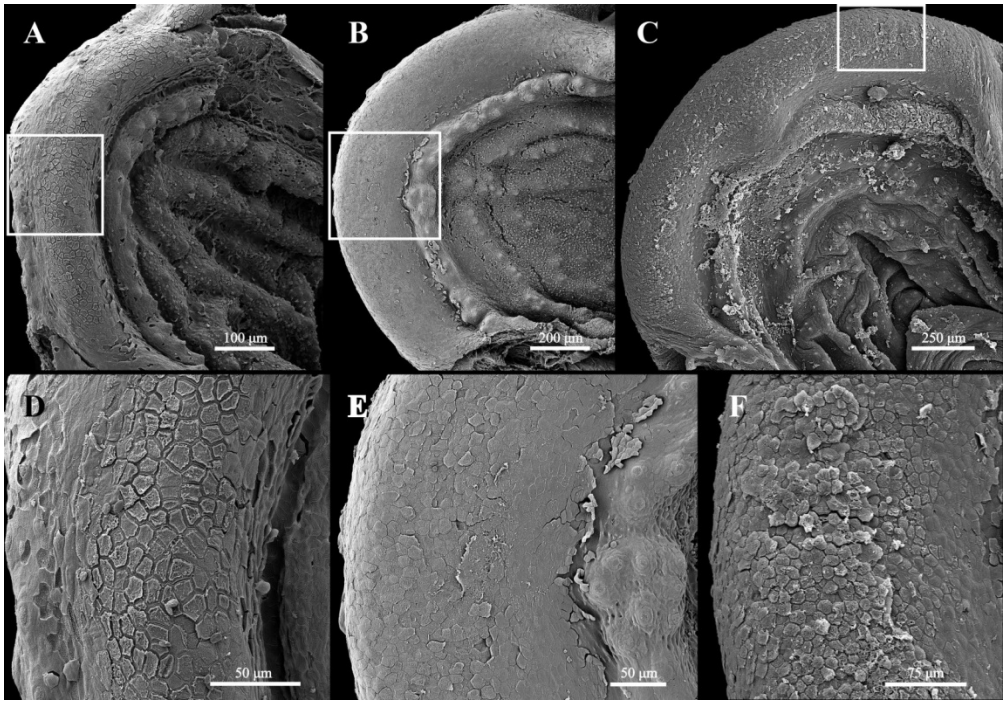

Figure 2-6. SEM photographs of the interior lower jaw epithelium of juvenile and adult *Dionda diaboli*. (**A**) Overview of unculi on a 25.0 mm SL juvenile. (**B**) Overview of flattened keratinized cells on a 6 month old hatchery-raised adult. (**C**) Overview of flattened keratinized cells on a wild-caught adult. (**D**) Close-up of solid box in A showing the still-raised, polygonal cells. (**E**) Close-up of the solid box in B showing the keratinized epithelium; raised unculi have been reduced to flattened, squamous-type cells. (**F**) Close-up of the solid box in C showing the similar keratinized squamous epithelium on the wild-caught specimen.

microplicae. Superficial cells of the epithelium covering the center of the upper and lower jaws exhibit a granular appearance due to the presence of multiple minute knob-like processes over the cell surface (Figure 2-5B). These cells lack the polygonal surface projection of cells located in a comparable position in smaller individuals, and contribute to a central transverse band that appears flaky in comparison to the smooth appearance of the epithelium located along the periphery of the jaws (Figure 2-6B-F). These granular superficial cells are arranged in a transverse band that covers approximately 44-58% and 62-65% of the upper and lower jaw epithelia, respectively (Table 2-1). The

granular cells stain intensely with eosin, indicating that they are keratinized. Cells of the epithelial layers immediately below the superficial layer of keratinized, granular cells in the transverse band to the basement membrane are cuboidal and do not stain with eosin (Figure 2-4D). The medial segment of the alimentary canal forms an anteriorly extended loop that is coiled multiple times inside of the boundary created by the outer loop. The anterior and posterior segments of the canal are straight and approximately equal in length.

2.3.8 Gut Elongation in Relation to Oral Keratinization

A strong positive correlation exists between gut length and standard length in *Dionda diaboli* (Figure 2-7). The area of keratinized epithelium covering the surface of the both the lower and upper jaw bones in *D. diaboli* also is strongly correlated with standard length (Figure 2-8, 2-9). The area of keratinized epithelium covering the surface of the lower jaw is consistently higher than that of the upper jaw (Figure 2-8, 2-9).

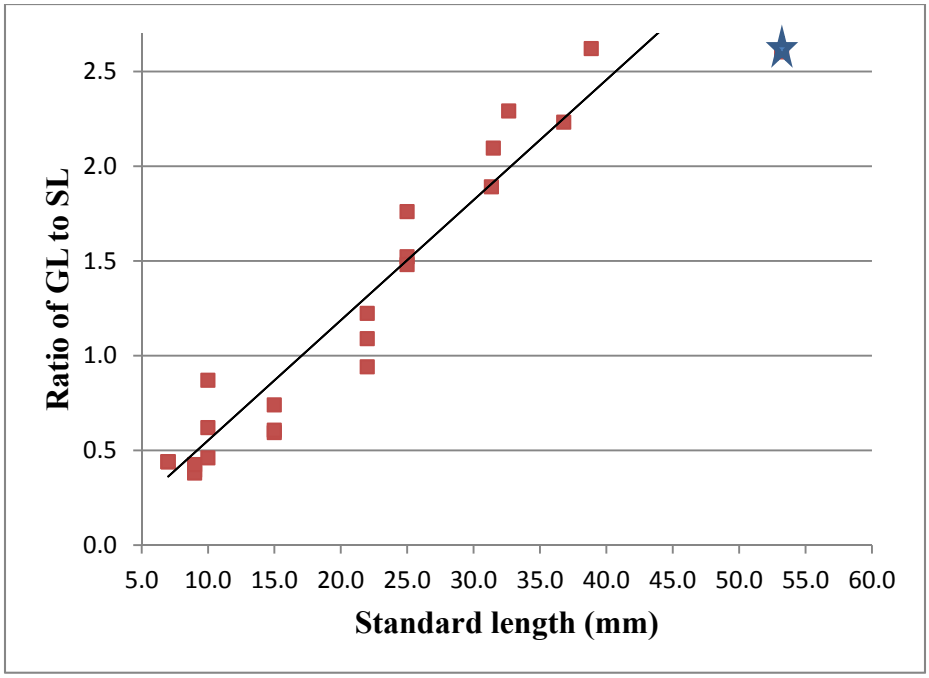

Figure 2-7. Gut length ratios correlated with standard lengths (mm) of larval, juvenile, and adult *Dionda diaboli.* Three individuals of each class had gut lengths examined. A star represents the single wild-caught adult specimen. $R^2 = 0.8808$.

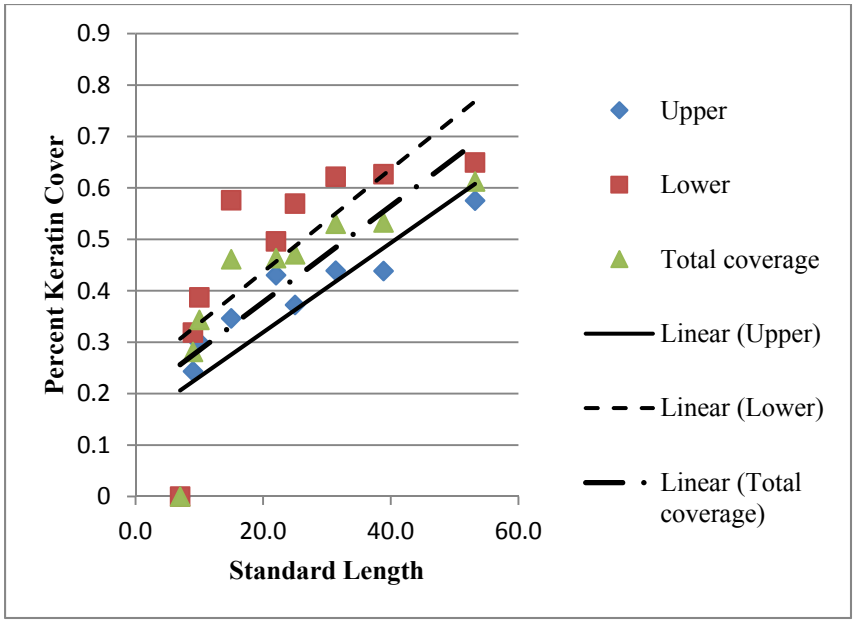

Figure 2-8. Ratios of keratin coverage among SEM individuals (n=1 per class) correlated with coinciding standard lengths (SL) (mm) for larval, juvenile, and adult *D. diaboli*. R^2=0.6912 (upper); R^2=0.5448 (lower); R^2=0.6237 (total coverage).

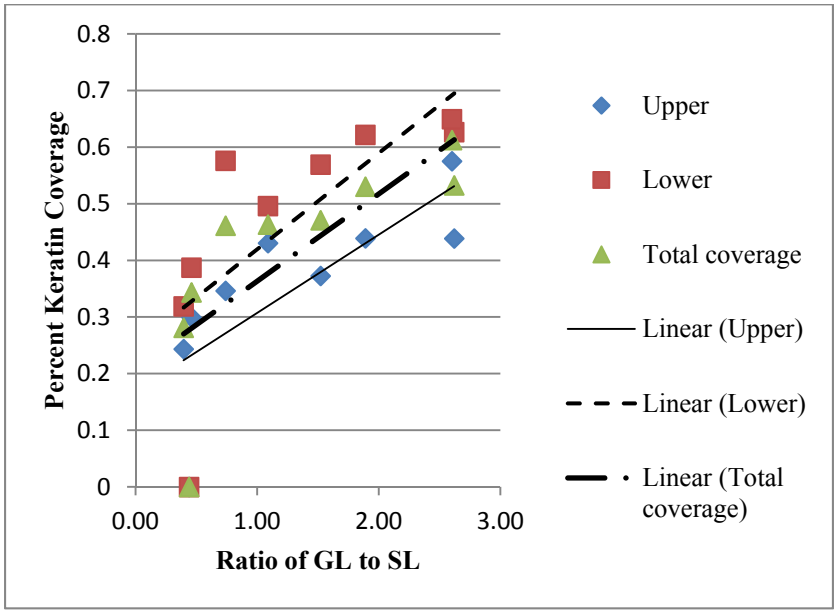

Figure 2-9. Correlation between oral keratin coverage and gut length (GL) ratio relative to standard length (SL) (mm) of individuals investigated via scanning electron microscopy. A total of 9 individuals were examined with upper, lower, and total keratin coverage for each individual shown as separate data points. R^2 =0.5881 (upper); R^2=0.5297 (lower); R^2=0.5706 (total coverage).

2.4 Discussion

2.4.1 Keratinized Oral Surfaces in Dionda diaboli

This investigation has documented the presence of keratin in the superficial cell layer of the epithelium covering the anteromedial surface of the jaw bones in the algivorous *Dionda diaboli*. As evidenced via histochemistry, keratin is present in this region of the trophic apparatus in all individuals ≥ 9 mm SL that were examined and absent only from individuals belonging to the smallest size class (7 mm SL) included for study. Signs of keratinization were first observed in individuals of 9 mm SL as a single transverse band of keratinized superficial cells at the center of the epithelium covering the surface of the jaw bones (Figure 2-2). In individuals of this size class, the transverse band of keratinized cells occupies an area covering approximately 20% and 30% of the surface of the epithelium surrounding the upper and lower jaw bones, respectively. As development proceeds, the transverse band of keratinized cells increase in width and length resulting in a broad band that covers approximately 50% and 60% of the surface of the epithelium surrounding the upper and lower jaw bones, respectively, in adult individuals (Table 2-1). It is likely that the earliest stages in the keratinization of the epithelium covering the jaw bones occurs at sizes between 7–9 mm SL and examination of additional individuals within this size range will be necessary to confirm this. Regardless of body size, once present, the transverse band of keratinized epithelium covering the lower jaw is consistently larger than that of the upper jaw. This pattern could result from keratinization initiating at an earlier stage in development within the

epithelium surrounding the lower jaw than the upper jaw or that the expansion of the keratinized epithelium occurs at a faster rate on the lower jaw than on the upper jaw. This pattern may also indicate a greater role for the lower jaw than the upper jaw during the process of substrate scraping.

In addition to changes in overall size, this study also documented ontogenetic changes in the appearance of the keratinized superficial cells that contribute to the transverse band of keratinized epithelia. In individuals of 9.0 mm SL the superficial cells contributing to the transverse band exhibit a large keratinous polygonal projection on the cell surface, which rises ~ 5-10 μm above the surface of the cell (Figure 2-3). Each keratinous projection exhibits a pronounced central concavity surrounded by a rugose margin, giving each projection a molar-like appearance (Figure 2-2). As body size increases, the height of the keratinous projection located at the surface of each superficial cell in the transverse band appears to decrease, as does the depth of the concavity located at the center of each projection until it is no longer obvious (Figure 2-5, 2-6). In the adult specimens examined, the keratinized superficial cells contributing to the transverse band lack a projection at the cell surface and instead exhibit a flattened surface with a granular texture (Figure 2-5, 2-6). These cells also lack the obvious polygonal shape of cells located in a similar position in smaller individuals, are extremely thin (2-4 μm), and appear to be easily sloughed from the surface (giving the surface of the transverse band a flaky appearance). Despite these differences, these cells stain positive for eosin as intensely as cells located in a similar position in smaller

individuals, which also stain deep red with A-S stain, and also are interpreted as keratinized.

Roberts (1982) introduced the term unculus (plural unculi) for a single keratinous projection arising from the surface of an epidermal cell in members of the Ostariophysi. Unculi are most commonly observed on surfaces that come into contact with the substrate, including the ventral surface of the head and body, ventral surface of the paired fins, and surfaces adjacent to or surrounding the mouth, including the lips, epithelia covering the surface of the jaw bones, and the rostral cap (Roberts 1982, Yashpal et al. 2009, Chuang et al. 2016, Geerinckx et al. 2007, Conway et al. 2012; Pinky et al. 2002, 2004). Unculi exhibit tremendous variation not only in overall size (ranging in height between 2-30 μm) but also in shape and surface ornamentation. To account for this variation, Roberts (1982) introduced a number of terms to describe the shape of unculi, including hemispherical, conical, polygonal truncate, hook-, leaf-, and tongue-shaped. The keratinous projections arising from the surfaces of the cells in the transverse band along the epithelium surrounding the upper and lower jaws in smaller individuals of *Dionda diaboli* (9.0-25.0 mm SL) match well with Roberts (1982) description of polygonal truncate unculi. Roberts (1982) documented polygonal truncate unculi on the epithelium covering the jaw bones (referred to as a horny sheath) in a number of North American minnows, including members of the genus *Semotilus* and *Nocomis*, and the archetypal North American algivore *Campostoma anomalum*. Pinky et al. (2002, 2004) reported polygonal-truncate unculi (referred to as "tooth-like" unculi) from the epithelia covering the jaw bones in the Old World cyprinid *Garra lamta*, and

Pinky & Mittal (2010) reported polygonal truncate unculi on the epithelia covering the jaw bones of *Puntius sophore,* which they referred to individually as "truncated, polygonal unculi" and collectively as a "horny-jaw sheath".

Previous histological investigations of the keratinized epithelium covering the jaw bones in the Old World cyprinids *G. lamta* (Pinky et al. 2002, 2004) and *P. sophore* (Tripathi & Mittal 2010) have shown that keratinization is restricted to the superficial unculiferous cell layer and is undetected in subjacent cell layers. A similar pattern of keratinization is present in the epithelium covering the jaw bones in *D. diaboli* regardless of body size. This pattern in which keratin is restricted to the superficial cell layer is similar to that present in the epidermis of some tetrapods (e.g., anurans) but differs drastically from other keratinized epithelia that have been investigated in fishes to date, in which keratinization extends through multiple cells tiers below the superficial layer. This includes (but is not restricted to) other unculiferous surfaces in otophysan fishes, including the paired-fins pads of cypriniform, siluriform, and characiform fishes (reviewed by Conway et al. 2012) and the adhesive apparatus of sisorid catfishes (Das & Nag 2004, 2005), and more complex keratinous structures, including the tubercles of cypriniform and siluriform fishes (Wiley & Collette 1970, Mittal & Whitear 1979) and the keratinous "teeth" surrounding the suctorial mouthparts of lampreys (Mittal & Whitear 1979, Uehara et al. 1983). In the aforementioned examples, the presence of keratin in multiple cells layers subjacent to the superficial layer may be reflective of the size and complexity of the keratinous structures themselves (i.e., the conical unculi that cover the surfaces of the adhesive apparatus of the sisorid catfishes are the tallest

reported to date). The restriction of keratinization to the superficial cell layer of the epithelium covering the jaw bones in many species of algivorous cyprinids (including *D. diaboli*) may indicate that the relatively short polygonal truncate unculi are produced relatively rapidly in the cell tier subjacent to the superficial layer. Additional investigation will be needed to confirm this and to further characterize the process of keratinization in the epithelium covering the surface of the jaw bones in algivorous minnows.

Roberts (1982) hypothesized that the "horny jaw sheaths" formed by fields of polygonal truncate unculi on the epithelium surrounding the jaw bones in many cyprinid fishes, including the North American archetypal algivore *Campostoma* (Matthews et al. 1987), are involved in abrasion of algae from the substrate. This study has provided further evidence in support of Roberts (1982) hypothesis by documenting vast fields of polygonal truncate unculi on the jaw epithelia in at least juvenile *Dionda diaboli.* The diversity of diets and trophic anatomy across North American minnows, including varying degrees of keratinization of the mouth parts (Gidmark & Simons 2014), offers an excellent opportunity to further test Roberts's (1982) hypothesis.

2.4.2 Keratinization and Gut Elongation

An elongate, coiled alimentary canal is typically associated with an algivorous or detritivorous diet involving the consumption of vast amounts of low nutrient forage and indigestible material. In contrast, fishes with omnivorous or carnivorous diets exhibit substantially shorter alimentary canals (German & Horn 2006, Kramer & Bryant 1995).

If polygonal truncate unculi on the jaw epithelia of algivorous fishes represent a modification for removing algae from the substrate one would expect the initiation of keratinization and the expansion of the keratinized epithelium in the mouthparts to occur concurrently with the process of gut elongation. As would be expected under this scenario, expansion of the keratinous transverse bands located in the epithelia surrounding the jaw bones was observed in concert with the elongation of the alimentary canal in *Dionda diaboli* (Figure 2-9). Interestingly, the greatest changes in gut length relative to body size (standard length) in *D. diaboli* occur between 9.0-10.0 mm and 15.0-25.0 mm SL, when the area covered by the transverse bands of keratinized epithelia on the jaws do not appear to increase rapidly. Conversely, the greatest changes in the extent of the keratinized epithelia covering the surface of the jaw bones occurred between size classes in which gut length did not increase greatly (7.0-9.0 mm and 10.0-15.0 mm SL) (Table 2-1).

The presence of keratinized transverse bands of polygonal truncate unculi in the epithelium covering the surface of the jaw bones in 9.0 mm SL individuals of *D. diaboli* may indicate that the ontogenetic dietary shift from planktivory to algivory is already underway far in advance of the first appearance of coils in the gut, which were not observed in individuals smaller than 22 mm SL (corresponding to approximately 32 DPH under hatchery conditions; Hubert et al. 2004) (Table 2-1). Hatchery programs attempting to rear *D. diaboli* have refined their methods for captive propagation (Gibson & Fries 2005) but mortality levels have remained high (Echo-Hawk 2015). The gradual

introduction of algae-based foods to the diet of hatchery fish that are approximately 9 mm SL could potentially result in improved yields of this threatened minnow.

CHAPTER III

NORTH AMERICAN ALGIVORES

3.1 Introduction

Keratinization of the epidermis is a well-documented feature among vertebrates (Alibardi 2009, Vandebergh & Bossuyt 2012). Although a keratinized epidermis is more frequently encountered among tetrapods, which may serve primarily as a means to avoid desiccation (Vandebergh & Bossuyt 2012), fishes are also capable of producing keratinized epithelia (Mittal & Whitear 1979, Mittal et al. 1995). The architecture of keratinized structures that are recorded among fishes vary immensely in shape, size, and complexity, ranging from tiny unicellular projections arising from the surface of a single cell (unculi *sensu* Roberts 1982) to larger multicellular structures such as tubercles (Wiley & Collette 1970) or the "teeth" of lampreys (Uehara et al. 1983). Unculi (singular unculus) were first described in detail by Roberts (1982) and documented from 16 families of the series Ostariophysi (the dominant group of freshwater fishes). Unculi exhibit considerable differences in size (ranging between 2-30 μm), shape (ranging from conical to polygonal), and surface microstructure, and are most commonly encountered on those parts of the body that regularly come into contact with the substrate, especially the ventral surface of the paired fins and the mouthparts (Roberts 1982, Geerinckx et al. 2007, Pinky et al. 2002, Conway et al. 2012).

Unculiferous surfaces are hypothesized to serve a number of different functions, including: adhesion, when located on the ventral surface of the body in rheophilic fishes (Chuang et al. 2016); or abrasion, when located on oral surfaces such as the lip or the epithelia covering the jaw bones in fishes that obtain food stuffs directly from the substrate (Pinky et al. 2002, Geerinckx et al. 2007, Roberts 1982). Recent functional investigations of unculi located on the ventral surfaces of the paired fins have provided strong evidence to support the role that unculi play in adhesion (Zou et al. 2016, Chuang et al. 2017). To the contrary, the abrasive properties of unculi located on oral surfaces have yet to be adequately explored and have been inferred based largely on scanning electron microscopy (SEM) examinations of Old World algivorous cyprinids, all of which exhibit vast fields of polygonal unculi on the lips and the epithelia covering the edentulous jaws (Roberts 1982, Tripathi & Mittal 2010, Yashpal et al. 2009). Comparable investigations in New World cyprinids are scarce and restricted to a small number of taxa, including the archetypal North American algivore *Campostoma*, in which unculi also are present in vast numbers on the epithelia covering the surface of the jaws (Roberts 1982). *Campostoma* belongs to a diverse clade of North American cyprinids (including nearly 300 species) which exhibit a variety of different diets, trophic anatomies and life history strategies (Gidmark & Simmons 2014). In addition to *Campostoma*, numerous other genera of North American cyprinid are comprised solely of obligate algivores, including members of *Achrocheilus*, *Dionda*, and *Hybognathus*, and some larger genera comprising primarily planktivores and omnivores also contain a small number of obligate algivores (e.g., *Notropis mekistocholas*). The high number of

obligate algivores (many of which are not closely related) in this clade of freshwater fishes presents an ideal opportunity to explicitly test the hypothesis that unculi situated on oral surfaces function as abrasive devices (Roberts 1982, Pinky et al. 2004).

In this study, I use a combination of SEM, histological techniques, and phylogenetic comparative methods to: (1) document the gross anatomy of the oral jaws in 55 species (representing 50 genera) of North American minnows; (2) characterize the nature and extent of oral keratinization; and (3) assess whether a relationship exists between oral keratinization and algivory in North American minnows.

3.2 Materials and Methods

3.2.1 Taxon Sampling

Specimens representing 55 species and 50 genera of North American minnows (Table 3-1) were obtained from museum collections and investigated using either scanning electron microscopy (SEM) and/or histological methods with light microscopy. This includes members of all genera of North American minnows recognized by Gidmark & Simons (2014), excluding *Aztecula*, *Luxilus*, *Moapa*, and *Klamathella*. The recent proposal to divide *Notropis* into multiple separate genera by Gidmark & Simons (2014) is not followed here.

Table 3-1. Material examined herein including cataloguing information.

Species	ID #	Museum
Acrocheilus alutaceus	OS 10672	Oregon State University Ichthyology Collection
Agosia chrysogaster	TCWC 16571.01	Biodiversity Research and Teaching Collections
Algansea tincella	TCWC 3082.01	Biodiversity Research and Teaching Collections
Campostoma anomalum	TCWC 16322.02	Biodiversity Research and Teaching Collections
Chrosomus erythrogaster	TCWC 6975.01	Biodiversity Research and Teaching Collections
Clinostomus elongatus	JFBM 46811	Bell Museum of Natural History
Codoma ornata	UMMZ 211133	University of Michigan Museum of Zoology
Codoma ornata	UF 10138	Florida Museum of Natural History
Couesius plumbeus	JFBM 47634	Bell Museum of Natural History
Cyprinella lutrensis	TCWC 16802.04	Biodiversity Research and Teaching Collections
Cyprinella venusta	TCWC uncat	Biodiversity Research and Teaching Collections
Dionda diaboli	TCWC uncat.	Biodiversity Research and Teaching Collections
Dionda sp.	TCWC 14782.01	Biodiversity Research and Teaching Collections
Dionda texensis	TCWC uncat.	Biodiversity Research and Teaching Collections
Eremichthys acros	JFBM 20946	Bell Museum of Natural History
Ericymba bucata	TCWC 17160.06	Biodiversity Research and Teaching Collections
Erimonax monachus	NCSM 61165	North Carolina Museum of Natural Sciences
Erimystax insignis	TCWC uncat.	Biodiversity Research and Teaching Collections
Exoglossum maxillingua	NYSM 69606	New York State Museum
Gila pandora	TCWC 15784.01	Biodiversity Research and Teaching Collections
Hemitremia flammea	JFBM 38353	Bell Museum of Natural History
Hesperoleucas symmetricus	TCWC 6924.02	Biodiversity Research and Teaching Collections
Hybognathus nuchalis	TCWC 14190.13	Biodiversity Research and Teaching Collections
Hybopsis amblops	UAIC 13270.04	University of Alabama Ichthyological Collection
Iotichthys phlegethontis	UMMZ 218947	University of Michigan Museum of Zoology
Lavinia excilicauda	LACM 35274-8	Natural History Museum of Los Angeles
Lepidomeda mollispinis	TCWC 3475.01	Biodiversity Research and Teaching Collections
Lythurus fumeus	TCWC 14727.03	Biodiversity Research and Teaching Collections
Machrybopsis aestivalis	TCWC 15553.06	Biodiversity Research and Teaching Collections
Margariscus margarita	TCWC 2678.01	Biodiversity Research and Teaching Collections
Meda fulgida	TCWC 3472.02	Biodiversity Research and Teaching Collections
Mylocheilus caurinus	OS 6159	Oregon State University Ichthyology Collection
Mylopharodon conocephalus	OS 4653	Oregon State University Ichthyology Collection
Nocomis asper	TCWC 6980.03	Biodiversity Research and Teaching Collections
Notemigonus crysoleucus	TCWC 14785.01	Biodiversity Research and Teaching Collections
Notropis hudsonius	TCWC 3181.09	Biodiversity Research and Teaching Collections
Notropis mekistocholas	NCSM 60995	North Carolina Museum of Natural Sciences
Opsopoeodus emiliae	TCWC 16899.11	Biodiversity Research and Teaching Collections

Table 3-1. Continued

Species	ID #	Museum
Oregonichthys kalawatseti	OS 11503	Oregon State University Ichthyology Collection
Orthodon macrolepitodus	OS 4654	Oregon State University Ichthyology Collection
Phenacobius mirabilis	TCWC 14223.01	Biodiversity Research and Teaching Collections
Pimephales promelas	TCWC 8020.06	Biodiversity Research and Teaching Collections
Pimephales vigilax	TCWC 16399.09	Biodiversity Research and Teaching Collections
Plagopterus argentissimus	UMMZ 217112	University of Michigan Museum of Zoology
Platygobio gracilis	JFBM 43259	Bell Museum of Natural History
Pogonichthys macrolepitodus	LACM 24971	Natural History Museum of Los Angeles
Pteronotropis welaka	TNHC 48864	Biodiversity Collections, University of Texas at Austin
Ptychocheilus oregonensis	OS 11096	Oregon State University Ichthyology Collection
Relictus solitarius	UMMZ 124955	University of Michigan Museum of Zoology
Rhinichthys cataractae	TCWC 15787.03	Biodiversity Research and Teaching Collections
Richardsonius balteus	TCWC 3470.01	Biodiversity Research and Teaching Collections
Semotilus atromaculatus	TCWC 15788.05	Biodiversity Research and Teaching Collections
Siphatelus bicolor	OS 9587	Oregon State University Ichthyology Collection
Tampichthys ipni	UMMZ 193492	University of Michigan Museum of Zoology
Tiaroga cobitis	TCWC 3472.03	Biodiversity Research and Teaching Collections
Yuriria alta	UMMZ 192267	University of Michigan Museum of Zoology

3.2.2 Scanning Electron Microscopy

The head from one individual of each species was separated from the body and dissected along the coronal plane into dorsal and ventral halves that included the upper and lower jaws, respectively. Division of the head commenced at the corners of the mouth and proceeded posteriorly through the junction of the ceratobranchials and epibranchials to expose the inner surfaces of the buccal cavity for examination using scanning electron microscopy (SEM). Dissected heads were chemically dried using the procedures of Ellis & Pendelton (2007), fastened to pin mounts with carbon tape, coated with gold in a Technics Hummer 1 vacuum sputter coater and observed using a

TESCAN Vega 3 environmental scanning electron microscope. Adobe Photoshop and Adobe Illustrator CS5.1 were used to process, edit, and analyze the resulting digital photographs.

3.2.3 Serial Sectioning

The head of two individuals representing select species (Table 3-2) were removed from the body and decalcified following Conway et al. (2012). Specimens were subsequently dehydrated through a series of EtOH and cleared in toluene before embedding in paraffin blocks. Embedded heads were sectioned sagittally (7 μm) utilizing a Spencer 820 rotary microtome. Sections were affixed to glass slides and stained with Ayoub-Shklar stain (A-S) for keratin following Ramulu et al. (2013) or hematoxylin and eosin (H&E) following the procedures of Kiernan (1990). Slides were observed and photographed using a ZEISS Primo Star compound light microscope outfitted with an AxioCam MRc5 digital camera. Adobe Photoshop and Adobe Illustrator CS5.1 were used to process, edit, and analyze the resulting digital photographs.

Table 3-2. Material examined using histology including catalogue ID.

Species	**Museum ID #**
Agosia chrysogaster	JFBM 18461
Alagansea tincella	TCWC 3082.01
Campostoma anomalum	TCWC 16322.02
Cyprinella lutrensis	TCWC 16802.04
Dionda diaboli	TCWC uncat.
Dionda texensis	TCWC uncat.

Table 3-2. Continued

Species	Museum ID #
Hesperoleucus symmetricus	TCWC 6924.02
Hybognathus nuchalis	TCWC 14190.13
Nocomis asper	TCWC 6980.03
Notropis hudsonius	TCWC 3187.09
Phenacobius mirabilis	TCWC 14223.01
Pimephales promelas	TCWC 8020.06
Richardsonius balteus	TCWC 3470.01

3.2.4 Gross Examination of the Alimentary Canal

The post-pharyngeal gut tract was separated from the body of dissected specimens and uncoiled if needed. Guts were measured (without stretching) to the nearest 0.1 mm using digital calipers. Alimentary tracts were classified based on the number of bends present as either s-shaped (two distinct bends occur) or coiled (multiple bends occur).

3.2.5 Phylogenetic Comparative Methods

A phylogenetic approach was used to assess whether an association exists between different aspects of keratinization of the epithelium covering the surface of the jaw bones and gut length (a proxy for algivory; German & Horn 2006). There is no available phylogenetic hypothesis inclusive of all genera of North American minnows and comparative analyses were based on two separate phylogenetic topologies that focused on different clades, including the 'shiner' clade (Hollingsworth et al. 2013) and the 'western' clade (Schönhuth et al. 2012). Prior to analyses, each phylogenetic

topology was pruned to include only those taxa examined herein using the "prune" function in Mesquite v.3.2 (Maddison & Maddison 2017). The resulting pruned topologies are provided in Appendix A. A small amount of overlap existed between the taxa present in each topology (e.g., *Exoglossum*) and this is the result of outgroup selection by the original authors (i.e., Hollingsworth et al. 2013 relied on members of the 'western' clade as outgroup taxa in their investigation of the 'shiner' clade and vice versa in Schönhuth et al. 2012). Due to the high number of taxa that had already been pruned from each topology, overlapping taxa were included in order to aid the preservation of original branch lengths (which were required for some of the comparative analyses).

A character matrix comprised of three binary characters was constructed to match the taxa present in each topology using MacClade v.4 (Maddison & Maddison 2000). Each matrix included three binary characters and two continuous characters. Binary characters included: (1) Diet: non-algivorous (state *0*); algivorous (state *1*); (2) Type of gut: s-shaped (state *0*); long, coiled (state *1*); and (3) Unculi: absent (state *0*); present (state *1*). Continuous characters included: (1) Ratio of gut length to standard length; and (2) percentage of keratin cover on lower jaw. The resulting matrices are provided in Appendix B. Binary characters were mapped on to each of the phylogenetic topologies using both MacClade and Mesquite. A Concentrated-changes test (Maddison 1990) was implemented in MacClade to test for the association of gut type (character 2) and each of the remaining characters (1, 3). The same associations between binary characters also were tested using Pagel's Correlation Test (Pagel 1994) in Mesquite. An

association between the two continuous characters was tested separately for each clade using Phylogenetic Independent Contrasts (Felsenstein 1985) and Phylogenetic Generalized Least Squares (Grafen 1989) was implemented in the statistical software R (R Core Team 2012) using the 'ape' (Paradis et al. 2004) and 'geiger' libraries (Harmon et al. 2008).

3.3 Results

3.3.1 Acrocheilus

There is no clear external demarcation between the lips and the skin covering the surface of the jaw bones in *A. alutaceus*. The skin covering the anterior margin of the lower jaw is greatly thickened, creating a broad, plate-like structure. Superficial cells of the epithelium covering the center of the lower jaw and the inner margin of the upper jaw appear rugose due to the presence of polygonal truncate unculi. The keratinized layer of cells is arranged in a transverse band that covers approximately 31% of the upper jaw and 76% of the lower jaw. The alimentary canal is long and coiled (Table 3-3).

Table 3-3. Summary of diet, gut type, gut length (provided as a ratio of GL to SL), epithelium type and percentage of keratinized epithelium on the surface of upper and lower jaws for taxa examined herein. A = algivorous.

Species	Gut Type	GL Ratio	Epithelium Type	% Keratin Cover		Diet
				Upper	Lower	
Acrocheilus alutaceus	coiled	1.247	keratinized squamous	0.314	0.756	A
Agosia chrysogaster	coiled	1.740	keratinized squamous	0.252	0.722	A
Algansea tincella	coiled	2.036	keratinized squamous	0.278	0.694	
Campostoma anomalum	coiled	4.075	unculiferous	0.614	0.784	A
Chrosomus erythrogaster	coiled	1.598	unculiferous	0.295	0.702	A
Clinostomus elongatus	s-shaped	0.737	keratinized squamous	0.451	0.597	
Codoma ornata	s-shaped	0.916	unculiferous	0.463	0.695	
Couesius plumbeus	s-shaped	0.920	keratinized squamous	0.427	0.728	
Cyprinella lutrensis	s-shaped	0.811	unculiferous	0.374	0.685	
Cyprinella venusta	s-shaped	0.586	unculiferous	0.409	0.704	
Dionda diaboli	coiled	2.602	keratinized squamous	0.650	0.705	A
Dionda sp.	coiled	2.306	keratinized squamous	0.560	0.684	A
Dionda texensis	coiled	2.234	keratinized squamous	0.460	0.585	A
Eremichthys acros	coiled	2.004	keratinized squamous	0.345	0.774	A
Ericymba bucata	s-shaped	0.891	keratinized squamous	0.280	0.714	
Erimonax monachus	s-shaped	0.759	keratinized squamous	0.275	0.833	
Erimystax insignis	s-shaped	0.791	keratinized squamous	0.275	0.717	
Exoglossum maxillingua	s-shaped	0.945	keratinized squamous	0.448	0.822	
Gila pandora	s-shaped	0.971	unculiferous	0.248	0.694	
Hemitremia flammea	s-shaped	0.907	unculiferous	0.467	0.711	
Hesperoleucas symmetricus	s-shaped	0.758	unculiferous	0.271	0.620	A
Hybognathus nuchalis	coiled	7.406	non-keratinized	0.000	0.000	A
Hybopsis amblops	s-shaped	0.597	keratinized squamous	0.284	0.551	
Iotichthys phlegethontis	s-shaped	0.848	keratinized squamous	0.562	0.745	
Lavinia excilicauda	coiled	2.954	unculiferous	0.272	0.757	
Lepidomeda mollispinis	s-shaped	0.739	keratinized squamous	0.308	0.786	
Lythurus fumeus	s-shaped	0.511	keratinized squamous	dmg	0.765	
Machrybopsis aestivalis	s-shaped	0.753	keratinized squamous	0.264	0.829	
Margariscus margarita	s-shaped	0.804	keratinized squamous	0.357	0.818	
Meda fulgida	s-shaped	0.654	keratinized squamous	0.325	0.830	
Mylocheilus caurinus	s-shaped	1.041	unculiferous	0.294	0.794	
Mylopharodon conocephalus	s-shaped	0.833	keratinized squamous	0.207	0.822	
Nocomis asper	s-shaped	0.793	unculiferous	0.252	0.793	
Notemigonus chrysoleucus	coiled	1.711	unculiferous	0.471	0.712	A
Notropis hudsonius	s-shaped	0.912	unculiferous	0.432	0.794	
Notropis mekistocholas	coiled	1.887	unculiferous	0.630	0.910	A
Opsopoeodus emiliae	s-shaped	0.697	unculiferous	0.511	0.821	
Oregonichthys kalawatseti	s-shaped	0.811	unculiferous	0.551	dmg	
Orthodon macrolepitodus	coiled	2.860	keratinized squamous	0.373	0.485	
Phenacobius mirabilis	s-shaped	0.804	keratinized squamous	0.203	0.845	
Pimephales promelas	coiled	3.846	unculiferous	0.459	0.744	
Pimephales vigilax	s-shaped	1.178	unculiferous	0.327	0.577	
Plagopterus argentissimus	s-shaped	0.920	keratinized squamous	0.247	0.782	

Table 3-3. Continued

Species	Gut Type	GL Ratio	Epithelium Type	% Keratin Cover Upper	% Keratin Cover Lower	Diet
Platygobio gracilis	s-shaped	0.911	unculiferous	0.333	0.795	
Pogonichthys macrolepitodus	s-shaped	1.113	keratinized squamous	0.162	0.331	
Pteronotropis welaka	s-shaped	0.807	unculiferous	0.403	0.856	
Ptychocheilus oregonensis	s-shaped	0.769	keratinized squamous	0.171	0.313	
Relictus solitarius	s-shaped	0.950	keratinized squamous	0.303	0.691	
Rhinichthys cataractae	s-shaped	0.783	unculiferous	0.209	0.854	
Richardsonius balteus	s-shaped	0.652	keratinized squamous	0.273	0.611	
Semotilus atromaculatus	s-shaped	0.776	unculiferous	0.321	0.788	
Siphatelus bicolor	s-shaped	1.009	unculiferous	0.470	0.692	
Tampichthys ipni	coiled	1.656	unculiferous	0.364	0.779	
Tiaroga cobitis	s-shaped	0.614	unculiferous	0.397	0.849	
Yuriria alta	s-shaped	0.824	keratinized squamous	0.385	0.664	

3.3.2 Agosia

There is no clear external demarcation between the lower lip and the skin covering the surface of the lower jaw in *A. chrysogaster*. A poorly developed groove is present between the upper lip and the skin covering the surface of the upper jaw at the symphysis. Superficial cells of the epithelium covering the center of the upper and lower jaws lack surface features and appear flaky when viewed with SEM. These cells stain intensely with eosin and stain bright red with A-S stain indicating that they are keratinized. Cells in layers subjacent to the keratinized superficial cell layer are cuboidal and show moderate eosin staining that remains uniform to within a few cell layers above the basement membrane (Figure 3-1C,D). The keratinized layer of cells is arranged in a transverse band that covers approximately 25% and 72% of the upper and lower jaw surfaces, respectively. The alimentary canal is long and coiled (Table 3-3).

3.3.3 Algansea

There is no clear external demarcation between the lips and the skin covering the surface of the jaw bones in *A. tincella*. Superficial cells of the epithelium covering the center of the lower jaw and the inner margin of the upper jaw appear flaky when viewed with SEM and exhibit rugged, coarse cell surfaces that lack microplicae. Rugged cells appear thickened and rectangular under light microscopy and stain intensely with both eosin and A-S stain, indicating the presence of keratin. The keratinized layer of cells is arranged in a transverse band that covers approximately 28% and 69% of the upper and lower jaw surfaces, respectively. The alimentary canal is long and coiled (Table 3-3).

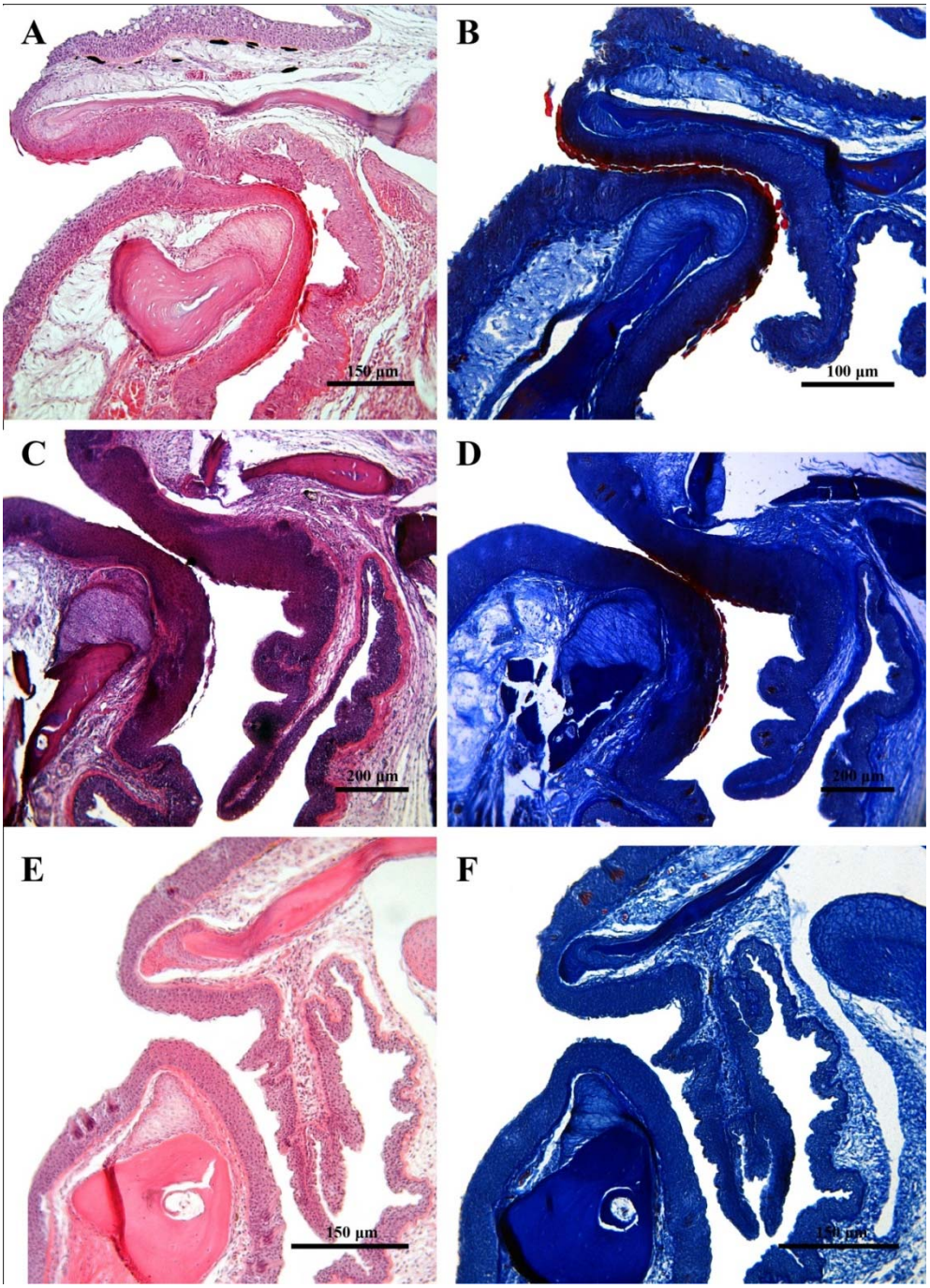

Figure 3-1. Sagittal sections through the buccal cavity in three species of North American minnows showing keratinized and non-keratinized epithelium. (**A**) *Dionda texensis*, 41.4 mm SL, stained with H&E. (**B**) *Dionda texensis* (same specimen in A), stained with A-S. (**C**) *Agosia chrysogaster*, 56.8 mm SL, stained with H&E. (**D**) *Agosia chrysogaster* (same specimen as in C) stained with A-S. (**E**) *Hybognathus nuchalis*, 46.6 mm SL, stained with H&E. (**F**) *Hybognathus nuchalis* (same specimen as in E) stained with A-S.

3.3.4 Campostoma

A poorly developed groove is present between the lower lip and the skin covering the lower jaw in *C. anomalum*. The upper lip is densely covered in taste buds and separated from the epithelium covering the jaw by a deep groove. The outermost epithelial layer on the entire sagittal curvature of the upper jaw and the center of the lower jaw consists of cells containing individual polygonal truncate unculi (Figure 3-2A,E; Figure 3-3A,B). The unculiferous cells form transverse bands that stain intensely with both eosin and A-S stain, indicating the presence of keratin. Directly subjacent cells in the second tier are rectangular and exhibit conspicuous counterstaining, indicating they are also keratinized. Remaining cell tiers down to the basement membrane are cuboidal and show moderate eosinophilia that declines with increasing proximity towards the basement membrane (Figure 3-3A,B). Keratinized, unculiferous cells cover an approximate 61% of the upper jaw and 78% of the lower jaw surface. The alimentary canal is long and coiled, and wound spirally around the gas bladder (Table 3-3).

3.3.5 Chrosomus

There is no clear external demarcation between the lower lip and the skin covering the surface of the lower jaw in *C. erythrogaster*. A poorly developed groove is present between the upper lip and the skin covering the surface of the upper jaw at the symphysis. The superficial epithelial cells on the inner curvature of the upper jaw and the center of the lower jaw appear rugose due to the presence of polygonal truncate unculi. The keratinized layer of cells is arranged in a transverse band that covers

approximately 30% and 70% of the upper and lower jaw surfaces, respectively. The alimentary canal is long and coiled (Table 3-3).

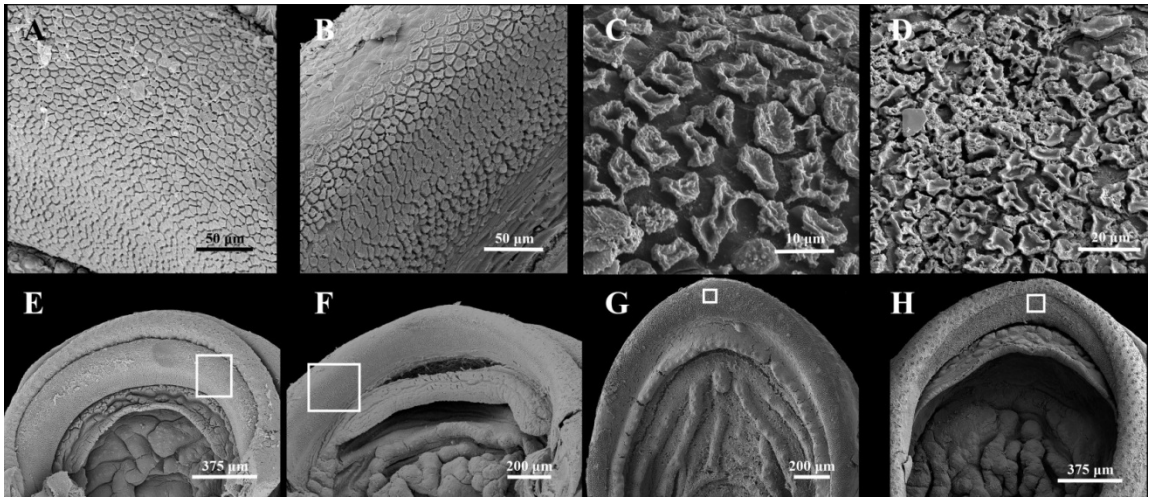

Figure 3-2. Scanning electron micrographs illustrating unculiferous jaw epithelia observed among North American minnows. (**A**) *Campostoma anomalum*, 34.8 mm SL, close-up of the solid box in E showing tall, stack-like unculi on the upper jaw. (**B**) *Pimephales promelas*, 35.4 mm SL, close-up of the solid box in F showing polygonal truncate unculi on the upper jaw. (**C**) *Pteronotropis walaka*, 42.1 mm SL, close-up of the solid box in G showing crenulated polygonal unculi on the lower jaw. (**D**) *Mylocheilus caurinus*, 42.3 mm SL, close-up of the solid box in H showing the highly crenulate unculi on the upper jaw. (**E**) *Campostoma anomalum* (same specimen as A), overview of the keratinized region on the inside of the upper jaw. (**F**) *Pimephales promelas* (same specimen as in B), overview of the keratinized area on the inside of the upper jaw. (**G**) *Pteronotropis welaka* (same specimen as in C), overview of the keratinized area on the inside of the lower jaw. (**H**) *Mylocheilus caurinus* (same specimen as in D), overview of the keratinized region on the inside of the upper jaw. Anterior to top of page.

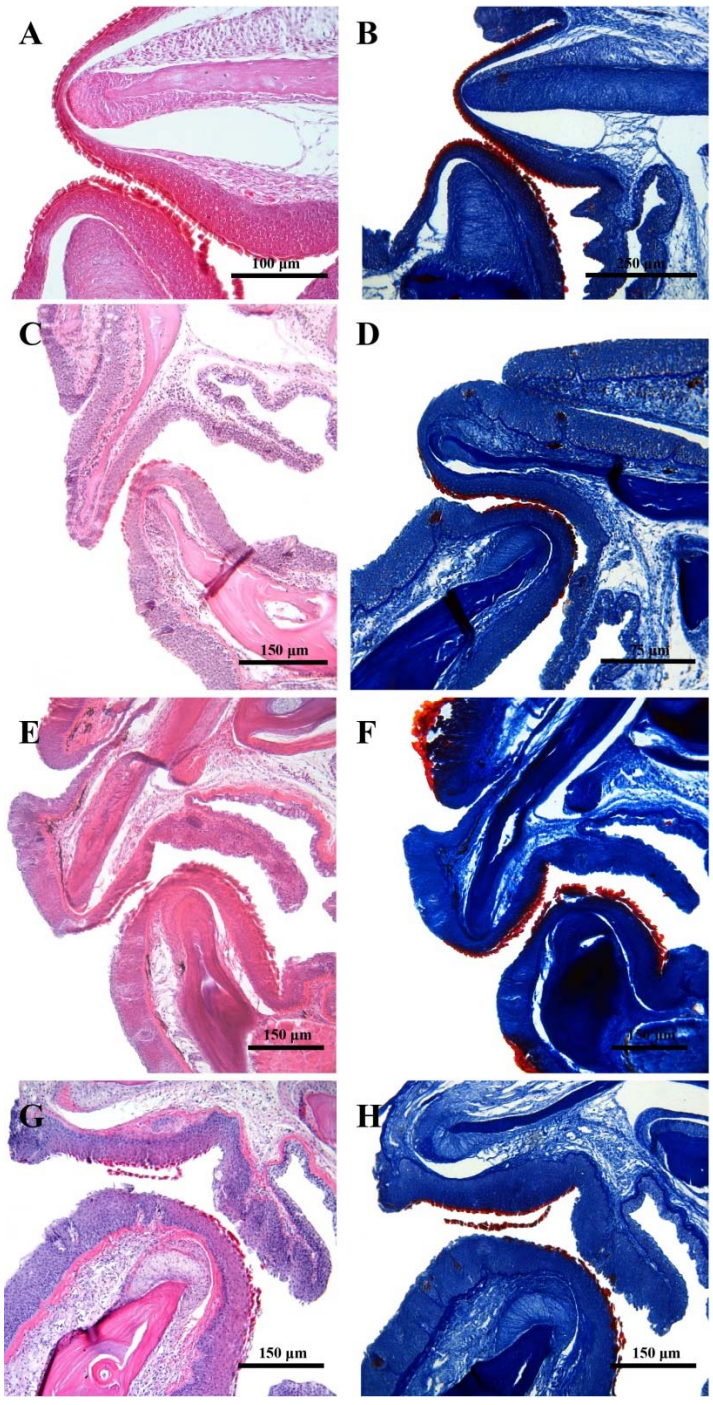

Figure 3-3. Sagittal sections through the buccal cavity in four species of North American minnows showing unculiferous epithelium. (**A**) *Campostoma* anomalum, 35.3 mm SL, stained with H&E. (**B**) *Campostoma anomalum* (same specimen as in A) stained with A-S. (**C**) *Pimephales promelas*, 33.0 mm SL, stained with H&E. (**D**) *Pimephales promelas* (same specimen as in C) stained with A-S. (**E**) *Cyprinella lutrensis*, 35.3 mm SL, stained with H&E. (**F**) *Cyprinella lutrensis* (same specimen as in E) stained with A-S. (**G**) *Notropis hudsonius*, 65.4 mm SL, stained with H&E. (**H**) *Notropis hudsonius* (same specimen as in G) stained with A-S.

3.3.6 Clinostomus

A poorly developed groove is present between the lower lip and the skin covering the lower jaw in *C. elongatus*; there is no obvious external demarcation between the upper lip and the skin covering the surface of the upper jaw. The superficial epithelial cells on the inner curvature of the upper jaw and the center of the lower jaw exhibit amorphous borders and non-uniform rugged surfaces composed of numerous knob-like microprojections. These cells appear flaky when viewed with SEM and form a transverse band that covers approximately 45% and 60% of the upper and lower jaw surfaces, respectively. The alimentary canal is S-shaped (Table 3-3)

3.3.7 Codoma

The upper and lower lips of *C. ornata* are each separated from the skin covering the jaw bones by a poorly developed groove that is most prominent at the symphysis of each jaw. Superficial epithelial cells covering the inner margin of the upper jaw and the center of the lower jaw possess polygonal truncate unculi with a singular central depression. Unculiferous cells are arranged in a transverse band that covers approximate 46% and 69% of the upper and lower jaw surfaces, respectively. The alimentary canal is S-shaped (Table 3-3).

3.3.8 Couesius

A poorly developed groove separates the upper lip from the skin covering the upper jaw in *C. plumbeus*; there is no obvious external demarcation between the lower

lip and the skin covering the lower jaw. The superficial epithelial cells within the inner curvature of the upper jaw and center of the lower jaw exhibit a cauliflower-like projection with numerous knobular microprojections and minute depressions over the surface. Cells with surface projections are arranged in a transverse band that covers approximately 43% and 73% of the upper and lower jaw surfaces, respectively. The alimentary canal is S-shaped (Table 3-3).

3.3.9 Cyprinella

There is no clear external demarcation between the lips and the skin covering the surface of the jaws in *C. lutrensis.* Superficial epithelial cells on the inner curvature of the upper jaw and center of the lower jaw exhibit polygonal truncate unculi each with a central concave depression. Unculi stain intensely with both eosin and A-S stain. Epithelial cells in the immediate underlying tier display a rectangular shape and also exhibit intense counterstaining, indicating keratinization. Remaining cell tiers down to the basement membrane are cuboidal and show counterstaining with eosin that remains moderate in intensity to within close proximity of the basement membrane (Figure 3-3E,F). Unculiferous cells are arranged in a transverse band that covers approximately 37% and 69% of the upper and lower jaw surfaces, respectively. The alimentary canal is S-shaped (Table 3-3).

In *Cyprinella venusta*, a weakly developed groove separates the lips from the skin covering the upper and lower jaws at the symphysis. Superficial epithelial cells covering the inner curvature of the upper jaw and the center of the lower jaw display

polygonal truncate unculi each containing a shallow central depression. Unculiferous cells are arranged in a transverse band that covers approximately 41% and 70% of the upper and lower jaw surfaces, respectively. The alimentary canal is S-shaped (Table 3-3).

3.3.10 Dionda

There is no clear external demarcation between the lips and the skin covering the surface of the jaws in *D. diaboli*. Superficial epithelial cells on the center of the lower jaw and the inner curvature of the upper jaw exhibit a flaky appearance under SEM, and display a coarse surface texture with numerous knobular microprojections. Superficial epithelial cells on the centers of the jaws stain intensely with eosin, indicating they are keratinized. Epithelial cells below the superficial layer are cuboidal, and cells in the second subjacent tier stain lightly with eosin while all other cell tiers remain basophilic down to the basement membrane. Keratinized cells are arranged in a transverse band that covers approximately 65% and 71% of the upper and lower jaw surfaces, respectively. The alimentary canal is long and coiled (Table 3-3).

In *Dionda sp*., a weakly developed groove separates the lips from the skin covering the upper and lower jaws at the symphysis. Superficial cells of the epithelium within the inner curvature of the upper jaw and at the center of the lower jaw display a weakly expressed polygonal shape with a rugged surface texture covered in numerous knob-like microprojections. Rugged superficial cells are arranged in a transverse band

that covers approximately 56% and 68% of the upper and lower jaw surfaces, respectively. The alimentary canal is long and coiled (Table 3-3).

There is no clear external demarcation between the lips and the skin covering the surface of the jaws in *D. texensis*. Superficial cells of the epithelium within the inner curvature of the upper jaw and center of the lower jaw appear flaky when viewed with SEM and exhibit coarse surfaces and amorphous cell borders (Figure 3-4A,E). Flaky superficial cells contain pyknotic nuclei and stain intensely with both eosin and A-S stain, indicating they are keratinized. Epithelial cells composing the second to fourth subjacent tiers are partially flattened and exhibit conspicuous though slightly less intense eosin counterstaining, indicating they contain keratin. Remaining cell tiers are cuboidal and show moderate eosinophilia that declines with increasing proximity towards the basement membrane (Figure 3-1A,B). Keratinized cells are arranged in a transverse band that covers approximately 46% and 58% of the upper and lower jaw surfaces, respectively. The alimentary canal is long and coiled (Table 3-3).

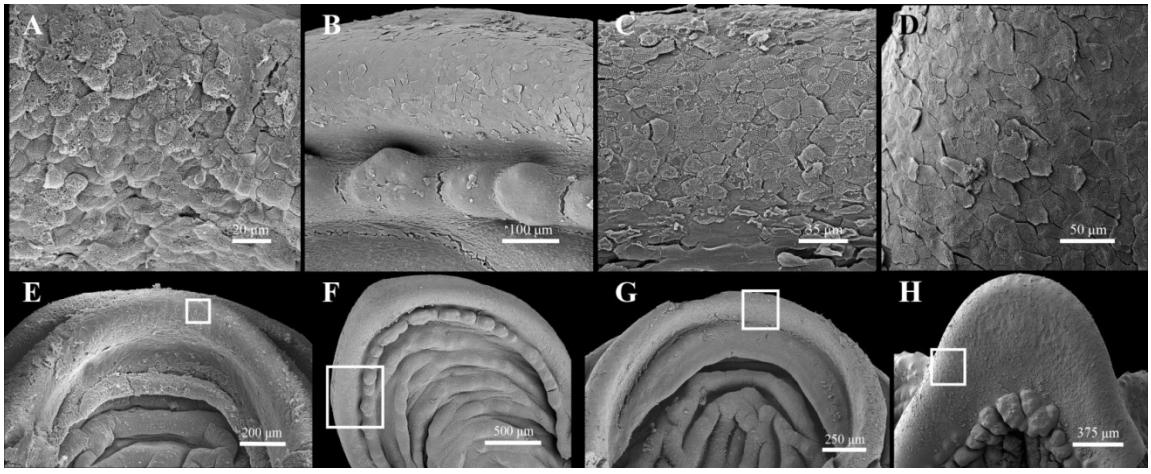

Figure 3-4. Scanning electron micrographs illustrating keratinized squamous jaw epithelia observed among North American minnows. (**A**) *Dionda texensis*, 39.5 mm SL, close-up of the solid box in E showing the thick, keratinized cells on the upper jaw. (**B**) *Richardsonius balteus*, 39.5 mm SL, close-up of the solid box in F showing the thin, keratinized cells on the lower jaw. (**C**) *Iotichthys phlegethontis*, 32.4 mm SL, close-up of the solid box in G showing the thick keratinized cells on the upper jaw. (**D**) *Exoglossum maxilligua*, 54.7 mm SL, close-up of the solid box in H showing the thin, keratinized cells on the lower jaw. (**E**) *Dionda texensis* (same specimen as in A), overview of the keratinized region on the inside of the upper jaw. (**F**) *Richardsonius balteus* (same specimen as in B), overview of the keratinized area on the inside of the lower jaw. (**G**) *Iotichthys phlegethontis* (same specimen as in C), overview of the keratinized region on the inside of the upper jaw. (**H**) *Exoglossum maxilligua* (same specimen as in D), overview of the keratinized area on the inside of the lower jaw. Anterior to top of page.

3.3.11 Eremichthys

In *Eremichthys acros*, the tissue belonging to the upper lip is separated from the skin covering the upper jaw by a deep groove; the lower lip is separated from the skin covering the lower jaw by a weakly developed groove. Superficial epithelial cells located on the inner curvature of the upper jaw and the center of the lower jaw are flaky in appearance when viewed under SEM and display lightly rugged surfaces covered with fine microprojections (Figure 3-5B,E). Rugged cells are arranged in a transverse band that covers approximately 34% and 77% of the upper and lower jaw surfaces, respectively. The alimentary canal is long and coiled (Table 3-3).

3.3.12 Ericymba

There is no clear external demarcation between the lips and the skin covering the surface of the jaws in *E. bucata*. Superficial epithelial cells on the inner arc of the upper jaw and center of the lower jaw display polygonal truncate unculi with each projection housing a single concave depression. Unculiferous cells are arranged in a transverse band that covers approximately 28% and 71% of the upper and lower jaw surfaces, respectively. The alimentary canal is S-shaped (Table 3-3).

3.3.13 Erimonax

The upper lip of *E. monachus* is fleshy, densely covered in taste buds, and separated from the skin covering the upper jaw by a well-developed groove. There is no visible external demarcation between the lower lip and the skin covering the lower jaw. Superficial epithelial cells in the inner curvature of the upper jaw and the center of the lower jaw exhibit polygonal truncate unculi with rugged margins and numerous knobular microprojections. Unculiferous cells are arranged in a transverse band that covers approximately 27% and 83% of the upper and lower jaw surfaces, respectively. The alimentary canal is S-shaped (Table 3-3).

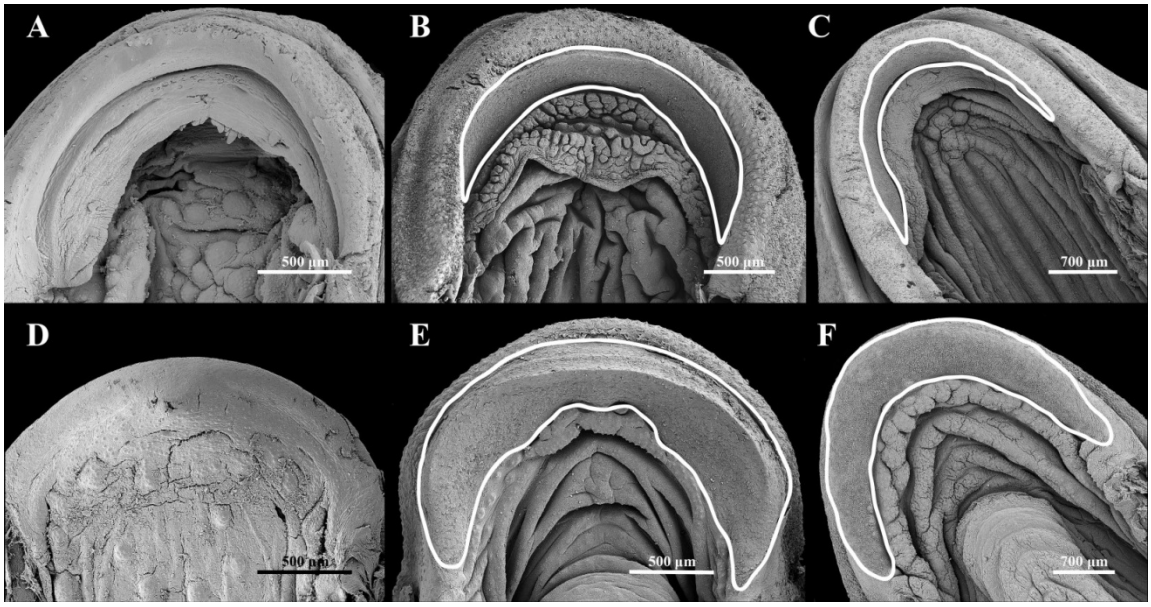

Figure 3-5. Scanning electron micrographs illustrating different states of keratinized jaw epithelia observed among North American minnows. (**A**) *Hybognathus nuchalis*, 48.4 mm SL, non-keratinized epithelium on inner surface of the upper jaw. (**B**) *Eremichthys acros*, 37.6 mm SL, keratinized squamous epithelium on inner surface of the upper jaw. (**C**) *Gila pandora*, 44.8 mm SL, unculiferous epithelium on inner surface of the upper jaw. (**D**) *Hybognathus nuchalis* (same specimen as in A), non-keratinized epithelium on surface of the lower jaw. (**E**) *Eremichthys acros* (same specimen as in B), keratinized squamous epithelium on surface of lower jaw. (**F**) *Gila pandora* (same specimen as in C), unculiferous epithelium on the surface of the lower jaw. Anterior to top of page. Keratinized epithelia outlined by a solid white line in B-C, E-F.

3.3.14 Erimystax

Weakly developed grooves separate the lips from the skin covering the upper and lower jaws in *E. insignis*. Taste buds on the inner periphery of the lower jaw occur on elongated, papillate stalks. Taste buds on the upper lip are densely located and each occurs on a raised, pyramidal papillum. Superficial cells of the epithelium within the center of the lower jaw and inner curvature of the upper jaw exhibit a weakly expressed polygonal truncate unculi with coarse, irregular outlines. Unculiferous cells are arranged

in a transverse band that covers approximately 28% and 72% of the upper and lower jaws, respectively. The alimentary canal is S-shaped (Table 3-3).

3.3.15 Exoglossum

In *E. maxillingua*, a weakly developed groove separates the upper lip from the skin covering the upper jaw. Deep vertical grooves transverse the entire upper lip and inner margin of the upper jaw. The lower lip is greatly reduced at the symphysis of the lower jaw, which is extended anteriorly into a broad triangular platform. Laterally, the lower lip is expanded into large, fleshy hemispherical lobes with numerous taste buds that flank the central triangular platform of lower jaw. The superficial cells of the epithelium covering the central part of the lower jaw and inner curvature of the upper jaw appear flaky and display lightly rugged surfaces with fine knobular microprojections (Figure 3-4D,H). These flaky cells cover approximately 45% and 82% of the upper and lower jaw surfaces, respectively. The alimentary canal is S-shaped (Table 3-3).

3.3.16 Gila

There is no clear external demarcation between the lips and the skin covering the surface of the jaws in *G. pandora.* Superficial cells of the epithelium on the interior curvature of the upper jaw and center of the lower jaw display polygonal truncate unculi that exhibit a single central depression or multiple depressions at the surface (Figure 3-5C,F). Unculiferous cells are arranged in a transverse band that covers approximately

25% and 69% of the upper and lower jaw surfaces, respectively. The alimentary canal is S-shaped (Table 3-3).

3.3.17 Hemitremia

There is no clear external demarcation between the lips and the skin covering the surface of the jaws in *H. flammea.* Superficial cells of the epithelium on the interior curvature of the upper jaw and the center of the lower jaw exhibit polygonal truncate unculi with rugose margins and a single central depression or multiple depressions at the surface. Unculiferous cells are arranged in a transverse band that covers approximately 47% and 71% of the upper and lower jaw surfaces, respectively. The alimentary canal is S-shaped (Table 3-3).

3.3.18 Hesperoleucas

There is no clear external demarcation between the lips and the skin covering the surface of the jaws in *H. symmetricus*. Superficial cells of the epithelium on the center of the lower jaw and interior arc of the upper jaw display polygonal truncate unculi that exhibit a single central depression or multiple depressions at the surface. Unculiferous cells are arranged in a transverse band that covers approximately 27% and 62% of the upper and lower jaw surfaces, respectively. The alimentary canal is S-shaped (Table 3-3).

3.3.19 Hybognathus

There is no clear external demarcation between the lips and the skin covering the surface of the jaws in *H. nuchalis* (Figure 3-5A,D). Intercellular borders between superficial cells of the epithelium on the anteromedial curvature of the upper jaw are weakly depressed compared to cell borders on other areas of the jaws. The epithelia covering the jaws is stratified squamous and lacks eosin or A-S counterstaining (Figure 3-1E,F), indicating the absence of keratinization. The alimentary canal is long and coiled (Table 3-3).

3.3.20 Hybopsis

Weakly developed grooves separate the lips from the skin covering the upper and lower jaws in *H. amblops*. Superficial cells of the epithelium on the center of the lower jaw and inner curvature of the upper jaw contain raised polygonal truncate unculi with irregular rugose edges. Unculiferous cells are arranged in a transverse band that covers approximately 28% and 55% of the upper and lower jaw surfaces, respectively. The alimentary canal is S-shaped (Table 3-3).

3.3.21 Iotichthys

There is no clear external demarcation between the upper lip and the skin covering the surface of the upper jaw in *I. phlegethontis*; a weakly developed groove separates the lower lip from the skin covering the lower jaw. Superficial cells of the epithelium on the center of the lower jaw and the interior curvature of the upper jaw

appear flaky under SEM with rugged, irregular cell surfaces due to the presence of numerous knobular microprojections (Figure 3-4C,G). Rugged cells are arranged in a transverse band that covers approximately 56% and 75% of the upper and lower jaw surfaces, respectively. The alimentary canal is S-shaped (Table 3-3).

3.3.22 Lavinia

There is no clear external demarcation between the lips and the skin covering the surface of the jaws in *L. excilicauda*. Superficial cells of the epithelium that are present in the center of the lower jaw and inner curvature of the upper jaw display low polygonal truncate unculi with irregular, rugged surfaces. Unculiferous cells are arranged in a transverse band that covers approximately 27% and 76% of the upper and lower jaw surfaces, respectively. The alimentary canal is long and coiled (Table 3-3).

3.3.23 Lepidomeda

Weakly developed grooves separate the lips from the skin covering the upper and lower jaws in *L. mollispinis.* Superficial cells of the epithelium present on the inner curvature of the upper jaw and the center of the lower jaw are weakly polygonal in shape with rugged surfaces caused by numerous knobular microprojections. These cells are arranged in a transverse band that covers approximately 31% and 79% of the upper and lower jaw surfaces, respectively. The alimentary canal is S-shaped (Table 3-3).

3.3.24 Lythrurus

There is no clear external demarcation between the lips and the skin covering the surface of the jaws in *L. fumeus*. The superficial epithelial cells on the center of the lower jaw and the interior curvature of the upper jaw display a polygonal shape with flat, lightly rugged surfaces covered in fine microprojections. These cells cover approximately 76% of the lower jaw. The upper jaw is partially damaged in individual examined and cell coverage could not be obtained. The alimentary canal is S-shaped (Table 3-3).

3.3.25 Machrybopsis

There is no clear external demarcation between the lips and the skin covering the surface of the jaws in *M. aestivalis*. Conspicuous mandibular barbels that are densely covered in taste buds are located at the lateral margins of the upper jaw. The superficial cells of the epithelium on the center of the lower jaw and the interior curvature of the upper jaw exhibit polygonal truncate unculi with a rugose surface that display a single central depression or multiple depressions. Unculiferous cells are arranged in a transverse band that covers approximately 26% and 83% of the upper and lower jaw surfaces, respectively. The alimentary canal is S-shaped (Table 3-3).

3.3.26 Margariscus

Weakly developed grooves separate the lips from the skin covering the upper and lower jaws in *M. margarita*. The superficial cells of the epithelium covering the center

of the lower jaw and the interior arc of the upper jaw exhibit a flaky appearance with lightly rugged surfaces covered in fine microprojections. Flaky superficial cells are arranged in a transverse band that covers approximately 36% and 82% of the upper and lower jaw surfaces, respectively. The alimentary canal is S-shaped (Table 3-3).

3.3.27 Meda

Weakly developed grooves separate the lips from the skin covering the upper and lower jaws in *M. fulgida*. Superficial cells of the epithelium on the central surface of the lower jaw and the inner curvature of the upper jaw are flaky in appearance with a rugged cell surface covered in thick knobular microprojections. Rugged cells are arranged in a transverse band that covers approximately 33% and 83% of the upper and lower jaws, respectively. The alimentary canal is S-shaped (Table 3-3).

3.3.28 Mylocheilus

A moderate groove separates the upper lip from the skin covering the upper jaw in *M. caurinus*; there is no clear external demarcation between the lower lip and the skin covering the lower jaw. The superficial epithelial cells present on the center of the lower jaw and the inner curvature of the upper jaw exhibit polygonal truncate unculi with a deep central depression (Figure 3-2D,H). Unculiferous cells are arranged in a transverse band that covers approximately 29% and 79% of the upper and lower jaw surfaces, respectively. The alimentary canal is S-shaped (Table 3-3).

3.3.29 Mylopharodon

A poorly developed groove separates the upper lip from the skin covering the upper jaw in *M. conocephalus*; there is no clear external demarcation between the lower lip and the skin covering the lower jaw. Epithelial cells in the outermost layer covering the center of the lower jaw and the inner curvature of the upper jaw display polygonal truncate unculi with a rugose surface that exhibit a single central depression or multiple depressions. Unculiferous cells are arranged in a transverse band that covers approximately 21% and 82% of the upper and lower jaw surfaces, respectively. The alimentary canal is S-shaped (Table 3-3).

3.3.30 Nocomis

A moderately developed groove separates the upper lip from the skin covering the upper jaw in *N. asper*; a weakly developed groove separates the lower lip from skin covering the lower jaw. Deep vertical grooves transverse the epithelia covering the central part of the upper and lower jaws; grooves appear deeper and more prominent along the inner curvature of the upper jaw. Superficial epithelial cells within the center of the lower jaw and the interior curvature of the upper jaw exhibit polygonal truncate unculi with rugose surfaces containing a central concave depression. Unculiferous cells stain intensely with eosin and A-S stain, indicating that they are keratinized. Epithelial cells in the two immediately subjacent tiers are rectangular and counterstain with identical intensity, indicating these layers also are keratinized. Remaining cell tiers are cuboidal and show moderate eosin staining that decreases in intensity to within a few

cell layers above the basement membrane. Unculiferous cells are arranged in a transverse band that covers approximately 25% and 79% of the upper and lower jaw surfaces, respectively. The alimentary canal is S-shaped (Table 3-3).

3.3.31 Notemigonus

There is no clear external demarcation between the lips and the skin covering the surface of the jaws in *N. crysoleucus*, Superficial epithelial cells on the center of the lower jaw and the inner curvature of the upper jaw exhibit polygonal truncate unculi with a rugose surface and a single central concavity. Unculiferous cells are arranged in a transverse band that covers approximately 47% and 71% of the upper and lower jaw surfaces, respectively. The alimentary canal is long and coiled (Table 3-3).

3.3.32 Notropis

Weakly developed grooves separate the lips from the skin covering the upper and lower jaws in *N. hudsonius*. Superficial epithelial cells that cover the center of the lower jaw and the interior curvature of the upper jaw exhibit polygonal truncate unculi with a rugose surface that exhibit a single central depression or multiple depressions. Unculiferous cells stain deep pink with eosin and bright red with A-S stain, indicating that they are keratinized. Epithelial cells in layers subjacent to the keratinized superficial cell layer are cuboidal and stain faintly with eosin to within a few cell layers above the basement membrane (Figure 3-3E,H). Unculiferous cells are arranged in a transverse

band that covers approximately 43% of the upper jaw and 79% of the lower jaw. The alimentary canal is S-shaped (Table 3-3).

Weakly developed grooves separate the lips from the skin covering the upper and lower jaws in *N. mekistocholas*. Epithelial cells of the superficial layer covering the interior curvature of the upper jaw and the central portion of the lower jaw exhibit raised polygonal unculi that each displays a weakly expressed singular concavity. Unculiferous cells are arranged in a transverse band that covers approximately 63% and 91% of the upper and lower jaw surfaces, respectively. The alimentary canal is long and coiled (Table 3-3).

3.3.33 Opsopoeodus

Weakly developed grooves separate the lips from the skin covering the upper and lower jaws in *O. emiliae*. Superficial epithelial cells that cover the central region of the lower jaw and the interior curvature of the upper jaw display polygonal truncate unculi that each displays a weakly expressed singular concavity. Unculiferous cells are arranged in a transverse band that covers approximately 51% and 82% of the upper and lower jaw surfaces, respectively. The alimentary canal is S-shaped (Table 3-3).

3.3.34 Oregonichthys

The lower jaw was damaged in the single individual of *O. kalawatseti* available for examination. A weakly developed groove separates the upper lip from the skin covering the upper jaw. Superficial cells of the epithelium lining the interior curvature of

the upper jaw display raised polygonal unculi with rugose surfaces and a singular central depression. The unculiferous cells cover approximately 55% of the upper jaw surface. The alimentary canal is S-shaped (Table 3-3).

3.3.35 Orthodon

There is no clear external demarcation between the lips and the skin covering the surface of the jaws in *O. macrolepitodus*. Superficial cells of the epithelium that cover the center of the lower jaw and the inner curvature of the upper jaw are flaky in appearance, with rugged surfaces containing irregular ridges and numerous knobular microprojections. Rugged epithelial cell are arranged in a transverse band that covers approximately 37% and 48% of the upper and lower jaw surfaces, respectively. The alimentary canal is S-shaped tube (Table 3-3).

3.3.36 Phenacobius

A moderately developed groove separates the upper lip from the skin covering the upper jaw in *P. mirabilis*. Well-developed vertical grooves transverse the upper lip, which is fleshy and densely covered with taste buds. There is no clear external demarcation between the lower lip and the skin covering the surface of the lower jaw. The superficial epithelial cells on the center of the lower jaw and the inner curvature of the upper jaw are flaky in appearance when viewed with SEM and exhibit coarse cell surfaces due to the presence of fine microprojections. The superficial cells of the epithelium contain pyknotic nuclei and stain intensely with eosin and A-S stain

indicating they are keratinized. Epithelial cells in layers beneath the keratinized superficial cell layer exhibit typical nuclei and are cuboidal. Eosin staining in subjacent cells tiers is moderate and decreases with increasing proximity towards the basement membrane. Keratinized cells are arranged in a transverse band that covers approximately 20% of the upper jaw and 85% of the lower jaw surfaces, respectively. The alimentary canal is S-shaped (Table 3-3).

3.3.37 Pimephales

There is no clear external demarcation between the lips and the skin covering the surface of the jaws in *P. promelas*. Superficial epithelial cells covering the center of the lower jaw and the inner margin of the upper jaw display polygonal truncate unculi each exhibiting a shallow, singular concavity (Figure 3-2B, F). The superficial epithelial layer stains intensely with eosin and A-S stain, indicating the cells are keratinized. Subjacent epithelial cell tiers down to the basement membrane stain basophilic with H&E (Figure 3-3C,D). Unculiferous cells are arranged in a transverse band that covers approximately 46% and 74% of the upper and lower jaw surfaces, respectively. The alimentary canal is long and coiled (Table 3-3).

There is no clear external demarcation between the lips and the skin covering the surface of the jaws in *P. vigilax*. The superficial cells of the epithelium covering the central region of the lower jaw and the interior curvature of the upper jaw appear rugose under SEM and display shallow polygonal truncate unculi. Unculiferous cells are

arranged in a transverse band that covers approximately 33% and 58% of the upper and lower jaw surfaces, respectively. The alimentary canal is S-shaped (Table 3-3).

3.3.38 Plagopterus

A moderately developed groove separates the upper lip from the skin covering the upper jaw in *P. argentissimus*; there is no external demarcation separating the lower lip from the skin covering the lower jaw. Superficial epithelial cells covering the center of the lower jaw and the inner margin of the upper jaw are rugged and flaky when viewed with SEM and cell surfaces are covered with numerous knobular microprojections. Rugged cells are arranged in a transverse band that covers approximately 25% and 78% of the upper and lower jaw surfaces, respectively. The alimentary canal is S-shaped (Table 3-3).

3.3.39 Platygobio

Weakly developed grooves separate the lips from the skin covering the upper and lower jaws in *P. gracilis*. Epithelial cells in the superficial layer on the central region of the lower jaw and the interior curvature of the upper jaw exhibit shallow polygonal truncate unculi that exhibit a single, shallow concavity at the surface. Unculiferous cells are arranged in a transverse band that covers approximately 33% and 80% of the upper and lower jaw surfaces, respectively. The alimentary canal is S-shaped (Table 3-3).

3.3.40 Pogonichthys

There is no clear external demarcation between the upper lip and the skin covering the surface of the upper jaw in *P. macrolepitodus*. A weakly developed groove separates the skin covering the lower jaw with that of the lower lip. The superficial cells of the epithelium covering the central part of the lower jaw and inner curvature of the upper jaw appear light flaky with extremely fine microprojections when viewed with SEM. Flaky epithelial cells cover approximately 18% and 33% of the upper and lower jaw surfaces, respectively. The alimentary canal is S-shaped (Table 3-3).

3.3.41 Pteronotropis

Weakly developed grooves separate the lips from the skin covering the upper and lower jaws in *P. welaka*. Superficial cells in the epithelium covering the center of the lower jaw and the inner curvature of the upper jaw exhibit polygonal truncate unculi that exhibit a deep central concavity at the surface (Figure 3-2C,G). Unculiferous cells are arranged in a transverse band that covers 40% and 86% of the upper and lower jaw surfaces, respectively. The alimentary canal is S-shaped (Table 3-3).

3.3.42 Ptychocheilus

A weakly developed groove separates the lower lip with the skin covering the lower jaw in *P. oregonensis*; no external demarcation is present between the upper lip and the skin covering the upper jaw. Superficial cells in the epithelium covering the center of the lower jaw and the inner curvature of the upper jaw appear flaky when

viewed with SEM and exhibit flat, relatively featureless surfaces. Flaky epithelial cells cover approximately 17% and 31% of the upper and lower jaw surfaces, respectively. The alimentary canal is S-shaped (Table 3-3).

3.3.43 Relictus

Weakly developed grooves separate the lips from the skin covering the upper and lower jaws in *R. solitarius.* The epithelial cells in the superficial layer covering the central region of the lower jaw and the inner curvature of the upper jaw are flaky in appearance when viewed with SEM and display rugged cell surfaces covered with numerous knobular microprojections. Rugged epithelial cells cover approximately 30% and 69% of the upper and lower jaw surfaces, respectively. The alimentary canal is S-shaped (Table 3-3).

3.3.44 Rhinichthys

The fleshy upper lip of *R. cataractae* is densely covered in taste buds and separated from the epithelium covering the lower jaw by a weakly developed groove. The anteromedial part of the upper lip is approximately twice as thick as those parts located laterally. There is no clear external demarcation between the lower lip and the skin covering the surface of the lower jaw. Superficial cells of the epithelium that are present on the interior curvature of the upper jaw and the center of the lower jaw appear rugose when viewed with SEM due to the presence of polygonal truncate unculi that exhibit a single central depression or multiple depressions at the surface. Unculiferous

cells cover approximately 21% and 85% of the upper and lower jaw surfaces, respectively. The alimentary canal is S-shaped (Table 3-3).

3.3.45 Richardsonius

Weakly developed grooves separate the lips from the skin covering the upper and lower jaws in *R. balteus.* Superficial cells of the epithelium present on the central region of the lower jaw and the interior curvature of the upper jaw are flaky in appearance when viewed with SEM and display lightly rugged surfaces with extremely fine microprojections (Figure 3-4B, F). Flaky superficial cells on the centers of the jaws stain bright pink with eosin and bright red with A-S stain, signifying that they are keratinized. Epithelial cell tiers directly subjacent to the superficial layer stain faintly with eosin and are strongly basophilic down to the basement membrane. Keratinized epithelial cells cover approximately 27% and 61% of the upper and lower jaw surfaces, respectively. The alimentary canal is S-shaped (Table 3-3).

3.3.46 Semotilus

Weakly developed grooves separate the lips from the skin covering the upper and lower jaws in *S. atromaculatus.* The superficial cells of the epithelium present at the center of the lower jaw and the inner curvature of the upper jaw appear rugose under SEM due to the presence of polygonal truncate unculi that exhibit a deep concavity at the surface. The unculiferous cells occupy approximately 32% and 79% of the upper and lower jaw surfaces, respectively. The alimentary canal is S-shaped (Table 3-3).

3.3.47 Siphatelus

There is no clear external demarcation between the lips and the skin covering the surface of the jaws in *S. bicolor*. The superficial cells of the epithelium in the center of the lower jaw and the interior curvature of the upper jaw exhibit raised polygonal unculi when viewed under SEM. Unculi display a rugose surface with one to multiple concavities. Unculiferous cells occupy approximately 47% and 69% of the upper and lower jaw surfaces, respectively. The alimentary canal is S-shaped (Table 3-3).

3.3.48 Tampichthys

A weakly developed groove separates the upper lip from the skin covering the upper jaw in *T. ipni*; there is no clear external demarcation between the lower lip and the skin covering the surface of the lower jaw. Superficial cells of the epithelium covering the inner curvature of the upper jaw and the central region of the lower jaw exhibit shallow polygonal truncate unculi that exhibit a simple rugged surface with or without a weak central concavity. Unculiferous cells occupy approximately 36% and 78% of the upper and lower jaws, respectively. The alimentary canal is long and coiled (Table 3-3).

3.3.49 Tiaroga

A weakly developed groove separates the upper lip from the skin covering the upper jaw in *T. cobitis*. There is no clear external demarcation between the lower lip and the skin covering the surface of the lower jaw. Superficial cells of the epithelium on the center of the lower jaw and the inner curvature of the upper jaw display rugose

polygonal truncate unculi that exhibit a single central depression or multiple depressions at the surface. Unculiferous cells cover approximately 40% and 85% of the upper and lower jaw surfaces, respectively. The alimentary canal is S-shaped (Table 3-3).

3.3.50 Yuriria

Weakly developed grooves separate the lips from the skin covering the upper and lower jaws in *Y. alta*. The inner curvature of the upper jaw exhibits several prominent vertical grooves. Superficial cells of the epithelium covering the center of the lower jaw and inner curvature of the upper jaw appear flaky when viewed with SEM and exhibit rugged cell surfaces covered in multiple knobular microprojections. Rugged cells are arranged in transverse bands that occupy approximately 39% and 66% of the upper and lower jaw surfaces, respectively. The alimentary canal is S-shaped (Table 3-3).

3.3.51 Phylogenetic Comparative Methods

Low probability scores (0.0-0.00047; Table 3-4) were obtained for the Concentrated-changes tests of algivory (character 1; state 1) against long coiled gut (character 2; state 2) for both the 'shiner' and 'western' clade datasets, suggesting that the changes in these characters are more concentrated along the same branches in each of the respective phylogenetic topologies than expected by chance alone (Maddison 1990). Similar results were obtained for Concentrated-changes tests of the character long coiled gut against the presence of unculi on the surface of the jaws (character 3; state 1) for the 'western' clade (probability 0.0; Table 3-4) but not for the 'shiner' clade (0.432;

Table 3-4) and so the null hypothesis (that changes in these two characters are distributed at random across this clade) could not be rejected. These results were mirrored by those obtained for Pagel's Correlation Test (Table 3-4).

Table 3-4. Summary statistics resulting from Correlated-character test (CC Test) and Pagel's Correlation Test (Pagle's λ) of binary characters and Phylogenetic Generalized-Least Squares (PGLS) and Phylogenetic-Independent Contrasts (PIC) for continuous characters conducted herein for both the 'shiner' and 'western' clades of minnows. Significant values are in bold and accompanied by an asterisk (*).

	CC Test	**Pagle's λ**				**PGLS**	**PIC**	
		4 Parameter model	**8 Parameter model**	**Difference in log likelihood**	**P value**		**r value**	**P value**
Shiner Clade								
Gut length/diet	**0.00047 4***	-30.2557619	-19.87108143	10.38468047	**0.0***	-	-	-
Gut length/unculi	0.432	-31.76886215	-31.53003417	0.238827985	0.82	-	-	-
Gut length/keratin cover on lower jaw	-	-	-	-	-	**0.00004**	0.338	**0.0***
Western Clade								
Gut length/diet	**0.0***	-27.71017663	-19.93327117	7.776905461	**0.0***	-	-	-
Gut length/unculi	**0.0***	-31.75670356	-29.02690374	2.729799822	**0.01***	-	-	-
Gut length/keratin cover on lower jaw	-	-	-	-	-	0.2367	0.05	0.2374

Both Phylogenetic independent-contrasts and Generalized-least squares analyses identified a significant correlation (P>0.0; Table 3-4) between gut length and the area of keratinized epithelium covering the surface of the jaws for members of the 'shiner' clade but not for the members of the 'western' clade, for which no significant correlation was detected between these two continuous characters (Table 3-4).

3.4 Discussion

3.4.1 Keratinized Oral Surfaces

This investigation has revealed that keratinization in the epithelium covering the surface of the jaw bones is a widespread phenomenon across North American minnows and occurs in taxa that exhibit a variety of different trophic morphologies, diets, and life histories. The majority of the taxa examined exhibited either well developed polygonal-truncate unculi on the epithelium covering the jaws or flat, squamous-type cells with rugged surfaces containing knobular microprojections that were also discovered (via histochemistry) to contain keratin. Of the 55 species examined, only one (*Hybognathus nuchalis*) exhibited no sign of keratinization (as evidenced by histochemistry) in the epithelium covering the surface of the jaw bones (Figure 3-1E,F), the cells of which appeared as typical squamous epithelial cells of the surface layer containing microplicae when observed with SEM (Figure 3-5A,D).

As for unculiferous cells, histochemical staining revealed that the squamous-type cells at the surface of the epithelium also contain keratin (Figure 3-1, 3-3). Regardless of

cell type (unculiferous vs. squamous-type), keratinization appears to be most commonly restricted to the superficial layer of the epithelium covering the surface of the jaw bones in the majority of species examined. The unculiferous epithelium in *Campostoma* and *Nocomis* is the only exception, as positive counterstaining for keratin extended beyond the superficial cell layer down to the second or third cell tier, though this appeared at varying intervals across each of these additional cell tiers. The location of the keratinized epithelium is also markedly consistent across the different taxa examined. On the lower jaw, the keratinized epithelium straddles the midline (jaw symphysis) and is located directly opposite to the keratinized epithelium on the inner arch of the upper jaw. The expanse of the keratinized epithelium (i.e., % of epithelium covering the surface of the jaw bones that is keratinized) also is consistently greater on the lower jaw than on the upper jaw. This observed pattern of coverage may indicate that the lower jaw is frequently exposed to higher abrasive contact and increased keratin cover is required on the lower jaw to facilitate improved protection or a more substantial gripping surface. The lack of keratinized epithelia on the oral jaws of *Hybognathus nuchalis* may indicate that this species exhibits a foraging behavior that avoids significant abrasive action on the jaws or potentially comes into contact only with soft substrates (e.g., soft detritus).

The surface architecture of non-unculiferous keratinized epithelial cells (squamous-type) was found to be highly variable across the 30 taxa that exhibited this characteristic (Figure 3-4, 3-1). In at least 10 species that display this type of epithelium, the surface texture of the keratinized cells is relatively smooth with fine microprojections, and the cells display a delicate flaky appearance when viewed with

SEM (Figure 3-4B,F,D,H). The remaining 20 species that display this character state exhibit superficial epithelial cells with an irregular, lightly ridged, or heavily knobbed surface texture with an overall heavier gestalt to the plate-like flakes on the jaws (Figure 3-4A,E,C,G). Further research is needed to clarify whether the squamous-type keratinized epithelial cells are different from unculiferous cells and do not simply represent unculiferous cells that have undergone abrasion. If this is shown to be true, the prevalence of these flattened yet keratinized cells in the superficial layer of the epithelium covering the surface of the jaw bones may be indicative of a heterogenous rate of cell turnover between the different species of North American minnows examined herein.

An unculiferous epithelium comprised of polygonal truncate unculi (Roberts 1982) was observed on the skin covering the jaw bones as a “horny sheath” in the remaining 25 species of North American cyprinid that were investigated in this study. The unculi that I have documented from the epithelia covering the jaw bones in different species are remarkably similar and show relatively minimal variation between species. In all cases, these unculi can be classified as polygonal truncate unculi (i.e., unculi with raised edges and a central concavity) (Figure 3-2) as described by Roberts (1982). Additional types of unculi described by Roberts (1982), including hemispherical, conical, leaf-, hook-, and tongue-shaped, were not observed on the epithelia covering the jaw bones in any of the taxa examined herein.

3.4.2 Dietary Correlates of Oral Keratinization

Elongation of the alimentary canal is a well-documented morphological phenomenon across algivorous fishes and is considered to represent an adaptation to improve digestive efficiency by increasing the retention time of low-nutrient forage within the gastrointestinal tract (German & Horn 2006). The strong correlation between an algivorous diet and a long, coiled alimentary canal in each of the clades of North American minnows ('shiner' clade and 'western' clade) investigated herein provides further support for this hypothesis. Along the same lines, an unculiferous epithelium covering the surface of the jaw bones also has been considered as a possible adaptation for algivory in edentulous fishes that must actively remove algae from the substrate without the aid of teeth (Roberts 1982). If credible, one would expect edentulous algivores (such as North American minnows) to be more likely to exhibit unculi on the surface of the jaw bones than non-algivores. This expectation is supported at least for the 'western' clade of North American minnows, in which the evolution of a long coiled gut (a proxy for algivory) and an unculiferous epithelium on the surface of the jaw bones appear to be tightly linked, but not for the 'shiner clade' in which the distribution of these two characters could not be distinguished from a random distribution (Table 3-4). The diversity of the 'shiner' clade is much greater than that of the 'western' clade and one possible reason for these disparate results could be a limited or biased sample of the members of this clade. For example, *Hybognathus* exhibits the highest ratio of GL to SL of all the taxa included in this study (Table 3-3) but is the only taxon to lack keratinization in the epithelium covering the surface of the jaw bones; the exact opposite

of what would likely be predicted *a priori* for this taxon. There is a strong possibility that *Hybognathus* has acted as an outlier in the analyses of the 'shiner' clade and affected the results of the character correlation tests. The same could be said for the results of the Phylogenetic Independent-Contrasts and Generalized-Least Squares analyses that identified a significant negative correlation between gut length and the area of keratinized superficial cells covering the surface of the lower jaw for the 'shiner' clade (Figure 3-6), which is the opposite of what would be expected if keratinization of the oral jaw epithelium was associated with algivory. Increasing the number of representatives of this clade included for analyses could help to alleviate the effects of "outliers" such as *Hybognathus* and provide a more thorough test of Roberts (1982) functional hypothesis on the role of unculi on oral surfaces.

The existence of well-developed unculi on the epithelium covering the surface of the jaw bones in many non-algivorous species of North American minnows may be indicative of a myriad of roles beyond abrasion for these tiny keratinous structures, including gripping or even the prevention of abrasions. For example, Adams et al. (2003) reported an oral grasping behavior at high water velocities among several species of lotic North American minnows, including members of *Cyprinella* and *Notropis*; non-algivorous taxa which have been shown herein to exhibit vast fields of unculi on the epithelia covering the surface of the jaws (Figure 3-3E-H). The abundance of highly crenulate unculi on the surface of the epithelium covering the jaws in many of the non-algivorous North American minnows examined herein could potentially assist the gripping of food items by the oral jaws prior to consumption or even the oral movement

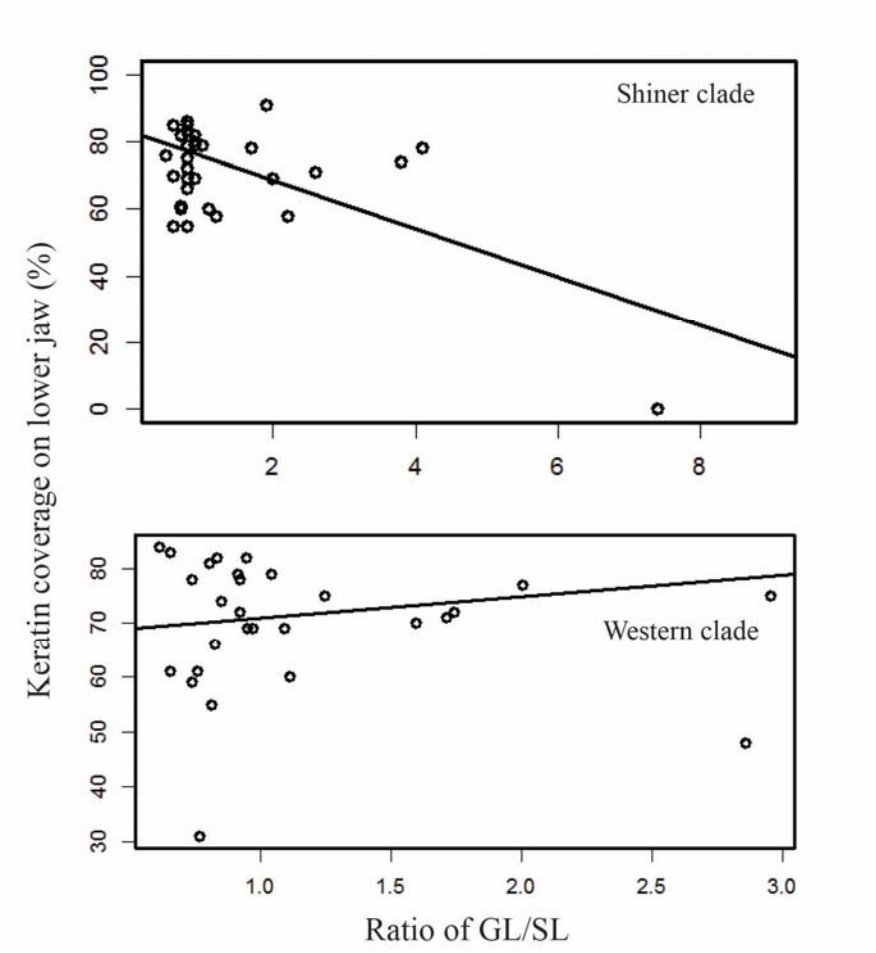

Figure 3-6. Relationship between ratio of gut length to standard length (GL/SL) to percentage of keratinized epithelium covering surface of lower jaw plotted as Phylogenetic Generalized Least Squares for members of the 'shiner' clade (upper) and 'western' clade (lower). See Table 3-4 for summary statistics.

of inedible items such as gravel or small peddles to build a spawning substrate as is characteristic of many North American cyprinid species, especially members of *Semotilus*, *Nocomis*, and *Exoglossum* (Johnston & Page 1992). To conclude, the role of keratinized epithelia covering the surface of the jaw bones in North American minnows

likely exceeds, though does not exclude, the scraping behavior associated with algivory in these edentulous fishes.

CHAPTER IV

CONCLUSION

The hypothesis of unculi as a scraping device arose from previous studies documenting an abundance of these structures on the oromandibular surfaces of African and Asian algivorous cyprinids, as well as the archetypal North American algivore *Campostoma*. Further investigation into this hypothesis was accomplished in the first segment of this study by documenting the presence and nature of keratinized oral surfaces in larvae, juveniles, and adults of the algivorous *Dionda diaboli* in conjunction with process of gut elongation (a clear adaptation for algivory). The second portion of this study was intended to further document the presence and nature of unculi on the trophic apparatus of many other North American species of cyprinids, and to assess whether this trait has evolved in concert with algivory across New World cyprinids, which would provide further insight into the function of unculi.

My investigation into the ontogeny of *D. diaboli* has revealed that development of a keratinized oral epithelium on the jaws occurs in concert with the elongation of the gut tract, and the discovery of unculi in individuals small as 9 mm could be interpreted as evidence to suggest that the algivorous diet of *D. diaboli* becomes established much earlier in the life history of this species than considered previously. The unculi observed are polygonal truncate in nature and exhibit a central concavity surrounded by a rugose margin, appearing molar-like, and the subsequent change in the height of unculi that

occurs as juveniles progress to adulthood may be due to the abrasive feeding behaviors of this species. Further investigation of individuals of *D. diaboli* would be needed to assess possible causes behind the transformation of these keratinized cells. The addition of algal matter into the diet of captive reared fry that are approximately 9 mm in length may increase rearing efficiency in hatchery programs, which is important for the long-term conservation of this species.

Additionally, my study revealed three character states of the jaw epithelium in North American minnows (non-keratinized, keratinized-squamous, and unculiferous) that were observed across 55 species and 50 genera. All North American minnows in this study, with the exception of *Hybognathus nuchalis*, possess either unculiferous or keratinized-squamous jaw epithelia and this feature does not appear to be significantly correlated with elongated gut tracts except among members of the 'Western' clade. However, the percentage of epithelial surface area that is keratinized on the jaws is negatively correlated with an elongated gut tract among members of the 'Shiner' clade. This negative correlation may be a product of the presence of *Hybognathus nuchalis* as an outlier given its unique combinations of characters (i.e., exceptionally long gut and non-keratinized jaw epithelia) and additional study would be needed to further assess the relationship between these characters within the 'Shiner' clade. Further study on the dietary habits of non-algivorous minnows in relation to the presence of unculi may reveal additional roles for these structures in the life history of these interesting fishes.

REFERENCES

Adams, S., G. L. Adams and J. J. Hoover. 2003. Oral grasping: A distinctive behavior of cyprinids for maintaining station in flowing water. Copeia, 2003(4): 851-857.

Alibardi, L. 2009. Embryonic keratinization in vertebrates in relation to land colonization. Acta Zoologica, 90: 1-17.

Cohen, K. L. 2008. Gut content and stable isotope analysis of exotic suckermouth catfishes (*Hypostomus*) in the San Marcos, TX: A concern for spring endemics (Thesis Dissertation). Texas State University.

Conway, K. W., N. K. Lujan, J. G. Lundberg, R. L. Mayden and D. S. Siegel. 2012. Microanatomy of paired fin-pads of Ostariophysan fishes (Teleostei: Ostariophysi). Journal of Morphology, 273: 1127-1149.

Chuang, Y., H. Chang, G. Liu and P. Chen. 2017. Climbing upstream: Multi-scale structural characterization and underwater adhesion of the Pulin river loach (*Sinogastromyzon puliensis*). Journal of the Mechanical Behavior of Biomedical Materials, available 23 January 2017. http://dx.doi.org.ezproxy.library.tamu.edu/10.1016/j.jmbbm.2017.01.029.

Das, D. and T. C. Nag. 2004. Adhesion by paired pectoral and pelvic fins in a mountain-stream catfish, *Pseudocheneis sulcatus* (Sisoridae). Environmental Biology of Fishes, 71: 1–5.

Das, D. and T. C. Nag. 2005. Structure of adhesive organ of the mountain-stream catfish, *Pseudecheneis sulcatus* (Teleostei: Sisoridae). Acta Zoologica, 86: 231–237.

Echo-Hawk, P. D. 2015. Performance of different diet types on larval rearing of the threatened Devils River minnow (*Dionda Diaboli*) (Thesis Dissertation). Texas A&M University Theses, Dissertations, and Records of Study (2002–).

Ellis, E. A. and M. W. Pendleton. 2007. Vapor coating: A simple, economical procedure for preparing difficult specimens for scanning electron microscopy. Microscopy Today, 17: 44.

Felsenstein, J. 1985. Phylogenies and the comparative method. American Naturalist, 125: 1–15.

Garret, G. P., C. Hubbs and R. J. Edwards. 2002. Threatened fishes of the world: *Dionda diaboli* Hubbs and Brown, 1956 (Cyprinidae). Environmental Biology of Fishes, 65: 478.

Garrett, G. P., R. J. Edwards and C. Hubbs. 2004. Discovery of a new population of Devils River minnow (*Dionda diaboli*), with implications for conservation of the species. The Southwestern Naturalist, 49(4): 435-441.

Geerinckx, T., J. De Poorter and D. Adriaens. 2007. Morphology and development of teeth and epidermal brushes in Loricariid catfishes. Journal of Morphology, 268: 805-814.

German, D. P. and M. H. Horn. 2006. Gut length and mass in herbivorous and carnivorous prickleback fishes (Teleostei: Stichaeidae): Ontogenetic, dietary, and phylogenetic effects. Marine Biology, 149: 1237–1245.

Gibson, J. R. and J. N. Fries. 2005. Culture studies of the Devils River minnow. North American Journal of Aquaculture, 67(4): 294-303.

Gibson, S. Z. 2015. Evidence of a specialized feeding niche in a late Triassic ray-finned fish: Evolution of multidenticulate teeth and benthic scraping in *Hemicalypterus*. The Science of Nature, 102(3-4): 1-7.

Gidmark, N. J. and A. M. Simons. 2014. Cyprinidae: Carps and minnows In: Freshwater fishes of North America, Petromyzontidae to Catostomidae, Vol. 1. Eds. M. L. Warren and B. M. Burr. Johns Hopkins University Press, Baltimore, MD.

Grafen, A. 1989. The phylogenetic regression. Philosophical Transactions of the Royal Society of London, Series B. Biological Sciences, 326(1233): 119-157.

Harmon, L. J, J. T. Weir, C. D. Brock, R. E. Glor and W. Challenger. 2008. GEIGER: investigating evolutionary radiations. Bioinformatics, 24: 129-131.

Hollingsworth, P. R., A. M. Simons, J. A. Fordyce and C. D. Hulsey. 2013. Explosive diversification following a benthic to pelagic shift in freshwater fishes. BMC Evolutionary Biology, 13(1): 272.

Hulbert, J., T. H. Bonner, J. N. Fries, G. P. Garrett and D. R. Pendergrass. 2004. Early development of the Devils River minnow, *Dionda diaboli* (Cyprinidae). The Southwestern Naturalist, 52(3): 378-385.

Johnston, C. E. and L. M. Page. 1992. The evolution of complex reproductive strategies in North American minnows (Cyprinidae) In: Systematics, historical ecology,

and North American freshwater fishes. Ed. R. L. Mayden. Stanford University Press, Sanford, CA.

Kiernan, J. A. 1990. Histological and histochemical methods: Theory and practice. 2nd ed. Oxford: Pergamon Press, New York.

Kramer, D. L. and M. J. Bryant. 1995. Intestine length in the fishes of a tropical stream: 2. Relationships to diet—the long and the short of a convoluted issue. Environmental Biology of Fishes, 42: 129–141.

Lopez-Fernandez, H., K. O. Winemiller and K. Bestgen. 2005. Status of *Dionda diaboli* and report of established populations of exotic fish species in lower San Felipe Creek, Val Verde county, Texas. The Southwestern Naturalist, 50(2): 246-251.

Maddison, W. P. 1990. A method for testing the correlated evolution of two binary characters: are gains or losses concentrated on certain branches of a phylogenetic tree?. Evolution, 44(3): 539-557.

Maddison, D. R. and W. P. Maddison. 2000. MacClade 4: Analysis of phylogeny and character evolution. Version 4.0. Sinauer Associates, Sunderland, Massachusetts.

Maddison, W. P. and D. R. Maddison. 2017. Mesquite: A modular system for evolutionary analysis. Version 3.2. http://mesquiteproject.org

Matthews, W. J., A. J. Stewart and M. E. Power. 1987. Grazing fishes as components of North American stream ecosystems: Effects of *Campostoma anomalum* In: Community and evolutionary ecology of North American stream fishes. Eds. W. J. Matthews and D. C. Heins. University of Oklahoma Press, Norman, OK.

Mittal, A. K. and M. Whitear. 1979. Keratinization of fish skin with special reference to the catfish *Bagarius bagarius*. Cell and Tissue Research, 202(2): 213-30.

Mittal, A. K., T. K. Garg and M. Verma. 1995. Surface architecture of the skin of the Indian catfish, *Bagarius bagarius* (Hamilton)(Sisoridae; Siluriformes). Japanese Journal of Ichthyology, 42(2): 187-191.

Pagel, M. 1994. Detecting correlated evolution on phylogenies: A general method for the comparative analysis of discrete characters. Proceedings of the Royal Society of London B, 255: 37-45.

Paradis, E., C. J. and K. Strimmer. 2004. APE: Analyses of phylogenetics and evolution in R language. Bioinformatics, 20: 289-290.

Pinky, S. M., J. Ojha and A. J. Mittal. 2002. Scanning electron microscopic study of the structures associated with the lips of an Indian hillstream fish *Garra lamta* (Cyprinidae, Cypriniformes). European Journal of Morphology, 40(3): 161-169.

Pinky, S. M., M. Yashpal, J. Ojha and A. K. Mittal. 2004. Occurrence of keratinization in the structures associated with lips of a hill stream fish *Garra lamta* (Hamilton)(Cyprinidae, Cypriniformes). Journal of Fish Biology, 65(4): 1165-1172.

R Core Team. 2012. R: A language and environment for statistical computing. R Foundation for Statistical Computing, Vienna, Austria. ISBN 3-900051-07-0. http://www.R-project.org/.

Ramulu, S., A. D. Kale, S. Hallikerimath and V. Kotrashetti. 2013. Comparing modified papanicolaou stain with ayoub‐shklar and haematoxylin‐eosin stain for demonstration of keratin in paraffin embedded tissue sections. Journal of Oral and Maxillofacial Pathology, 23(1): 23-30.

Roberts, T. R. 1982. Unculi, (horny projections arising from single cells), an adaptive feature of the epidermis of Ostariophysan fishes. Zoologica Scripta, 11(1): 55-76.

Schönhuth, S., D. K. Shiozawa, T. E. Dowling and R. L. Mayden. 2012. Molecular systematics of western North American cyprinids (Cypriniformes: Cyprinidae). Zootaxa, 3586(28): 1-303.

Snelson Jr., F. F. 1971. *Notropis mekistocholas*, a new herbivorous cyprinid fish endemic to the Cape Fear River basin, North Carolina. Copeia, 1979(3): 449-462.

Tripathi, P. and A. K. Mittal. 2010. Essence of keratin in lips and associated structures of a freshwater fish *Puntius sophore* in relation to its feeding ecology: Histochemistry and scanning electron microscope investigation. Tissue and Cell, 42: 223-233.

Uehara, K., S. Miyoshi and H. Toh. 1983. Fine structure of the horny teeth of the lamprey, *Entosphenus japonicas*. Cell Tissue and Research, 231: 1-15.

Uehara, K. and S. Miyoshi. 1993. Structure of comblike teeth of the ayu sweetfish, *Plecoglossus altivelis* (Teleostei: Isospondyli): I. Denticles and tooth attachment. Journal of Morphology, 217(2): 229-238.

Vandebergh, W. and F. Bossuyt. 2012. Radiation and functional diversification of alpha keratins during early vertebrate evolution. Molecular Biology and Evolution, 29(3): 995-1004.

Wiley, M. L. and B. B. Collette. 1970. Breeding tubercles and contact organs in fishes: Their occurrence, structure and significance. Bulletin of the American Museum of Natural History, 143: 146-216.

Yamaoka, K. 1983. Feeding behaviour and dental morphology of algae scraping cichlids (Pisces: Teleostei) in Lake Tanganyika. African Study Monographs, 4: 77-89.

Yashpal, M., U. Kumari, S. Mittal and A. K. Mittal. 2009. Morphological specializations of the buccal cavity in relation to the food and feeding habit of a carp *Cirrhinus mrigala*: A scanning electron microscopic investigation. Journal of Morphology, 270: 714-728.

Zou, J., J. Wang and C. Ji. 2016. The adhesive system and anisotropic shear force of Guizhou Gastromyzontidae. Scientific Reports, 6: 37221.

APPENDIX A

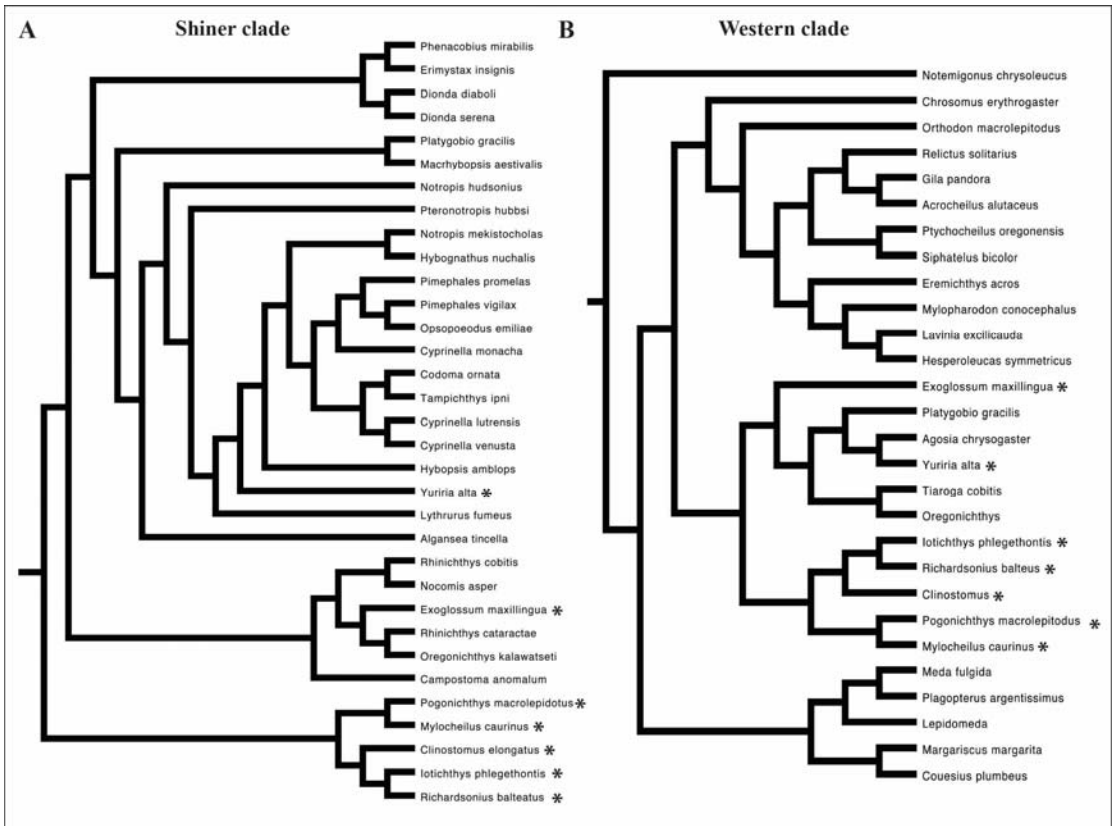

A-1. Pruned phylogenetic topologies utilized for tests of character correlation and phylogenetic comparative analyses in this study. (**A**) 'Shiner' clade from Hollingworth et al. (2013; Figure 3-2). (**B**) 'Western' clade from Schonhuth et al. (2012; Figure 3-2). Asterisks (*) indicate taxa common to both topologies.

APPENDIX B

Taxon	Algivory	Gut type	Unculi	Ratio of GL/SL	% Keratin (lower jaw)
Agosia_chrysogaster	1	1	1	1.7	72
Algansea_tincella	0	1	1	2.0	69
Campostoma_anomalum	1	1	1	4.1	78
Clinostomus_elongatus	0	0	1	0.7	60
Codoma_ornata	0	0	1	0.9	69
Cyprinella_lutrensis	0	0	1	0.8	69
Cyprinella_monacha	0	0	1	0.8	83
Cyprinella_venusta	0	0	1	0.6	70
Dionda_diaboli	1	1	1	2.6	71
Dionda_serena	1	1	1	2.2	58
Erimystax_insignis	0	0	1	0.8	72
Exoglossum_maxillingua	0	0	1	0.9	82
Hybognathus_nuchalis	1	1	0	7.4	0
Hybopsis_amblops	0	0	1	0.6	55
Iotichthys_phlegethontis	0	0	1	0.8	75
Lythrurus_fumeus	0	0	1	0.5	76
Macrhybopsis_aestivalis	0	0	1	0.8	83
Mylocheilus_caurinus	0	0	1	1.0	79
Nocomis_asper	0	0	1	0.8	79
Notropis_hudsonius	0	0	1	0.9	79
Notropis_mekistocholas	1	1	1	1.9	91
Opsopoeodus_emiliae	0	0	1	0.7	82
Oregonichthys_kalawatseti	0	0	1	0.8	55
Phenacobius_mirabilis	0	0	1	0.8	85
Pimephales_promelas	0	1	1	3.8	74
Pimephales_vigilax	0	0	1	1.2	58
Platygobio_gracilis	0	0	1	0.9	80
Pogonichthys_macrolepidotus	0	0	1	1.1	60
Pteronotropis_hubbsi	0	0	1	0.8	86
Rhinichthys_cataractae	0	0	1	0.8	85
Rhinichthys_cobitis	0	0	1	0.6	85
Richardsonius_balteatus	0	0	1	0.7	61
Tampichthys_ipni	0	1	1	1.7	78
Yuriria_alta	0	0	1	0.8	66

B-1. Data matrix of continuous and binary characters for species examined in the ‘Shiner’ clade.

Taxon	Algivore	Gut Type	Unculi	GL/SL Ratio	% Keratin (lower jaw)
Acrocheilus_alutaceus	1	1	1	1.3	76
Agosia_chrysogaster	1	1	1	1.7	72
Chrosomus_erythrogaster	0	1	1	1.6	70
Clinostomus_elongatus	0	0	1	0.7	60
Couesius_plumbeus	0	0	1	0.9	73
Eremichthys_acros	1	1	1	2	77
Exoglossum_maxillingua	0	0	1	0.9	82
Gila_pandora	0	0	1	1	69
Hesperoleucas_symmetricus	1	0	1	0.8	62
Iotichthys_phlegethontis	0	0	1	0.8	75
Lavinia_excilicauda	0	1	1	2.9	76
Lepidomeda	0	0	1	0.7	79
Margariscus_margarita	0	0	1	0.8	82
Meda_fulgida	0	0	1	0.7	83
Mylocheilus_caurinus	0	0	1	1	79
Mylopharodon_conocephalus	0	0	1	0.8	79
Notemigonus_crysoleucus	1	1	1	1.7	71
Oregonichthys	0	0	1	0.8	55
Orthodon_macrolepitodus	0	1	1	2.9	48
Plagopterus_argentissimus	0	0	1	0.9	78
Platygobio_gracilis	0	0	1	0.9	80
Pogonichthys_macrolepitodus	0	0	1	1.1	33
Ptychocheilus_oregonensis	0	0	1	0.8	31
Relictus_solitarius	0	0	1	0.9	69
Richardsonius_balteus	0	0	1	0.7	61
Siphatelus_bicolor	0	0	1	1.1	69
Tiaroga_cobitis	0	0	1	0.6	85
Yuriria_alta	0	0	1	0.8	66

B-2. Data matrix of continuous and binary characters for species examined in the ‘Western’ clade.